Honours Thesis

In vitro selection of DNA aptamers that neutralise autoantibodies to cytosolic 5'-nucleotidase-1A

Nataliya Slater

This thesis is presented for the degree of Bachelor of Science Honours, School of Veterinary and Life Sciences, of Murdoch University, 2019

Total word count: 21,834
Manuscript word count (including headings and subheadings): 19,186

Murdoch
UNIVERSITY

Declaration.

I declare that this thesis is my own account of my research and contains as its main content work which has not previously been submitted for a degree at any tertiary education institution.

Candidate: Nataliya Slater

Date: 21 October 2019

Copyright Acknowledgement.

I acknowledge that a copy of this thesis will be held at the Murdoch University Library.

I understand that, under the provisions of s51.2 of the Copyright Act 1968, all or part of this thesis may be copied without infringement of copyright where such a reproduction is for the purposes of study and research.

This statement does not signal any transfer of copyright away from the author.

Signed:

Full Name of Degree:	Bachelor of Science with Honours in Biomedical Science
Thesis Title:	*In vitro* selection of DNA aptamers that neutralise autoantibodies to cytosolic 5'-nucleotidase-1A
Author:	Nataliya Slater
Year:	2019

Acknowledgements.

I wish to extend my sincere gratitude to my Honours supervisor, Dr Jerome Coudert, for being entirely invested in the success of my project and his unwavering belief in my capabilities. Jerome always had his door open when I needed guidance whilst allowing me the freedom to follow my scientific curiosity.

I must also thank my second supervisor, Dr Rakesh Veedu, and his team including Tao and Hadi, who were all incredibly generous with their time and offered invaluable technical assistance and advice about aptamers and SELEX.

I am grateful to Prof Merrilee Needham and Kelly Beer, who have been vital for acquiring IBM sera samples for the project. Thank you both for attending the research update meetings and providing your valued feedback on my presentations. Also, thank you, Merrilee, for assisting with the poster printing.

I am thankful to Christine Bundell at PathWest for her assistance with the ELISA protocol and healthy sera samples. Your collaboration was invaluable in the early stages of this project.

I wish to thank everyone at the Institute for Immunology and Infectious Diseases for their willingness to share their extensive knowledge and for making me feel an integral part of the team.

I want to acknowledge Murdoch University for providing the project and personal financial assistance via Murdoch University Honours Allowance and Honours Academic Excellence Award.

The Honours experience would not have been as enjoyable and memorable without my fellow students and friends, Emily and Jose. I feel truly fortunate to have worked alongside you and to have shared all the highs and lows of research.

I am endlessly grateful to my families in Ukraine and Australia. I am blessed to have parents who placed high value on education and encouraged me to keep learning throughout life. Thank you for supporting me in my many endeavours.

The completion of my thesis would not have been possible without my husband's unreserved support. Thank you, Phil, for rearranging your days and taking on home duties so that I could spend extra time in the lab and write on weekends. And thank you for believing in me when I was doubting myself.

Thanks to my kids, Sophie and William, for unknowingly giving me the inspiration to do my very best every day.

I am indebted to my family-in-law and friends who helped me balance parenting and full-time Honours workload. Special thanks to Barbara, whose flexibility and generosity with her time enabled this to happen.

It is true that without all the love, care, guidance and support by all those people around me, completing my Honours would have been a grueling task. In this case, my success is your success also. Thank you.

Table of Contents

List of Figures.

List of Tables.

List of Equations.

Abbreviations.

ALS	amyotrophic lateral sclerosis
BCA	bicinchoninic acid
BCR	B cell receptor
BSA	bovine serum albumin
cN1A	cytosolic 5'-nucleotidase-1A
(d)PAGE	(denaturing) polyacrylamide gel electrophoresis
DM	dermatomyositis
DTT	dithiothreitol
ELISA	enzyme-linked immunosorbent assay
Fab	fragment antigen-binding
Fc	fragment crystallisable
HRP	horseradish peroxidase
Ig	immunoglobulin
IIM	idiopathic inflammatory myopathies
IMAC	immobilised metal-affinity chromatography
PCR	polymerase chain reaction
PM	polymyositis
RCF	relative centrifugal force
RPM	rotations per minute
SDS	sodium dodecyl sulphate
SELEX	systematic evolution of ligands by exponential enrichment
TMB	3,3,5,5-tetramethylbenzidine

Abstract.

Background. Inclusion Body Myositis (IBM) is the most commonly diagnosed inflammatory muscle disease associated with aging. It's characterised by degeneration of skeletal muscles that inevitably leads to the loss of mobility. The mechanisms that drive IBM pathogenicity remain poorly understood. However, studies reveal that on average 50% of IBM sera contains circulating autoantibodies targeting cytosolic 5'-nucleotidase 1A (cN1A) – a metabolic enzyme that is highly expressed in skeletal muscles. Accumulating evidence suggests that anti-cN1A antibodies may play a role in IBM pathogenesis making them an attractive target for aptamer development.

Problem. IBM remains refractive to current immunosuppressive treatments. Preventing anti-cN1A antibodies binding to their target protein may reduce the severity of IBM symptoms and halt the disease progression.

Aim. Within this project, we aim to select DNA aptamers that conjugate with anti-cN1A binding sites and prevent their interaction with cN1A protein.

Results. Sera of forty-eight IBM patients were screened with enzyme-linked immunosorbent assay (ELISA) against purified cN1A protein. Eighteen patients (38%) were found seropositive. 6.5 mg of polyclonal anti-cN1A were purified out of 90 ml of a selected IBM patient's blood. Their biological activity against cN1A was confirmed by ELISA.

Purified anti-cN1A were used as a target for aptamer selection. Initial library of single-stranded DNA fragments (aptamers) was synthesised with a 40-nucleotide randomised region flanked by constant primer-binding sites. Neutralising aptamers were selected through the process of systematic evolution of ligands by exponential enrichment (SELEX). Two complete cycles of selection against anti-cN1A were performed. Selected aptamers were assayed for their neutralising capacity by ELISA. Anti-cN1A were pre-incubated with the aptamers at various concentrations. Following a one-hour incubation, the ELISA-obtained absorbance remained unchanged or increased in a dose-dependent manner. While upon an extended overnight

incubation, a 25% decrease in absorbance values corresponding to a 35% decrease in anti-cN1A binding was observed.

Conclusions. The methodology developed during this project resulted in the generation of aptamers that conjugate with anti-cN1A binding sites. Following two SELEX cycles, the selected aptamers demonstrate 35% neutralisation capacity upon prolonged incubation with the immunoglobulins. Our results strongly suggest that the aptamers target monomeric IgG and IgA while having low or no affinity for IgM anti-cN1A.

CHAPTER 1. Introduction: inclusion body myositis, cytosolic 5'-nucleotidase-1A antibodies and DNA aptamers.

1.1. Clinicopathological features, population prevalence and diagnosis of inclusion body myositis.

Idiopathic inflammatory myopathies (IIM), also referred to as "autoimmune myositis" or simply "myositis", are a heterogeneous group of disorders that affect skeletal muscles as well as many organs, such as the heart, lungs, and skin.[1] Inflammatory myopathies can be divided into subgroups based on a patient's clinical presentation and laboratory findings. Most commonly, IIMs are grouped into dermatomyositis (DM), polymyositis (PM), necrotising autoimmune myopathy, anti-synthetase syndrome, overlap syndrome myositis and inclusion body myositis (IBM).

IBM is the most frequently diagnosed myopathy in adult patients over 40 years of age.[2] It affects proximal and distal muscles of arms and legs, notably finger and wrist flexors and quadriceps.[3] Other muscle groups, such as spinal, facial, and oropharyngeal, can also be affected to various degrees.[4] The symptoms of asymmetric muscle weakness often more pronounced in the non-dominant side develop slowly but inevitably progress.[4] The reported average rate of muscle strength loss is between 3.5 and 5.5% per year.[4, 5] Although IBM is not inherently life-threatening, it can significantly reduce the quality of life as patients become reliant on mobility assistance within on average 15 years from the onset of the symptoms.[5] Furthermore, difficulty swallowing (dysphagia) causing malnutrition, as well as reduced respiratory function often associated with advanced disease can reduce IBM patients' life expectancy comparing to general population.[6]

IBM prevalence varies with geographical location. In Northern Europe, the number of IBM cases has been estimated between 4.9 per million of population in the Netherlands[7] to 33 per million in Norway.[8] Data from Japan indicates a lower but increasing incidence of 10 per million.[9] In Western Australia, the number of IBM cases was 9.3 per million in 2000.[10] However, in patients

over 50 years of age, the prevalence of the disease is much higher at 51.3 cases per million.[11] Importantly, these statistics are likely to be underestimated due to the long asymptomatic period of the condition, an average delay of 4.4 years between the onset of symptoms and diagnosis,[10] and a high rate of misdiagnosis, as the clinical presentation of IBM can be attributed to other myopathies, typically polymyositis, as well as some categories of amyotrophic lateral sclerosis (ALS).[12]

J. Mendell proposed that most if not all IBM cases can be diagnosed from a muscle biopsy based on the presence of certain pathological features.[3] Known as "Griggs" criteria, *definite* IBM is diagnosed when a patient's muscle biopsy shows evidence of mononuclear cell invasion of nonnecrotic muscle fibres, contains rimmed vacuoles, and either amyloid deposits or 15- to 18-nm tubulofilaments, regardless of the clinical presentation.[3] However, it is not unusual, especially in the early-stage disease, that the biopsy doesn't show all of these features. Such cases are diagnosed as *possible* IBM or often polymyositis that clinically resembles IBM. In a retrospective follow-up study of 165 patients with either a previous diagnosis of myositis or clinical features of muscle weakness, nine patients were initially diagnosed with polymyositis using clinical, laboratory, and histopathologic criteria.[13] Upon follow-up, five of the nine patients showed characteristic features of IBM.[13] The distinction between IBM and polymyositis is especially important, since IBM is retractive to glucocorticosteroidal or immunomodulating treatments that are effective in polymyositis patients.[14] Thus, experts agree that early and accurate diagnosis of a patient presenting with muscle weakness is of the prime importance to their prognosis, treatment prescription and possible involvement in clinical trials.[15] For this reason, the inclusion of additional serologic markers in the diagnostic criteria for IBM is being investigated.[15, 16]

This review summarises the current knowledge of one such serologic marker, a recently discovered autoantibody against cytosolic 5'-nucleotidase 1A, and its role in IBM diagnosis, pathology, and treatment.

1.2. Humoral immunity.

1.2.1. B cells, plasma cells, and antibodies.

Antibodies, also classified as immunoglobulins (Ig) due to their globular structure, are an essential functional protein of the adaptive immune system. In healthy individuals, they confer protection against pathogens through immobilisation of microorganisms, and neutralisation of viral activity and toxins. An antigen is any part of a pathogen or a substance that evokes an immune response. Bacterial and viral antigens are generally contained in the extracellular fluids; thus, the immune response against them is called humoral immunity (from *Latin*, "humor" meaning "fluid").

Antibodies can be bound to the surface of B cells where they serve the role of antigen-specific receptors called BCRs. Every individual generates a vast repertoire of BCR antigen specificities, which almost guarantees a response to any antigen that they might encounter in their lifetime. In fact, the BCR antigen variability is so extensive that most B cells never encounter their matching antigen and remain naïve B cells.

Those B cells that interact with their corresponding antigen will terminally differentiate into plasma cells that secrete antibodies. To date, two pathways of B cell activation have been described. In a T-cell independent response, B cells react with bacterial antigens such as bacterial cell wall components and polysaccharides and do not require additional signals from T-lymphocytes to activate.[17] In a classic T cell-dependent antigen-driven immune response, B cells activated by a protein antigen migrate to lymph nodes and spleen where they receive a second activation signal from a CD4+ "helper" T cell reactive to amino acid fragments (epitopes)

derived from the same antigenic protein.[17] Only T-cell dependent activation is thought to result in production of memory B cells and long-lived antibody-producing plasma cells.[17]

Each plasma cell secretes antibodies of a single antigenic specificity, the same specificity as the BCR on the surface of the B cell that produced it. However, a strong response to a single antigen typically involves a polygenic antibody response where a population of plasma cells produce antibodies reactive to different epitopes of the same antigen.

1.2.2. Antibody structure.

The structure of an immunoglobulin molecule was first determined in 1959 when treatment with papain split it into three segments of approximately the same size: two retained the ability to bind antigen and were referred to as Fab (fragment antigen-binding); while the third could be crystallised out of the solution and was termed Fc (fragment crystallisable) (Figure 1).

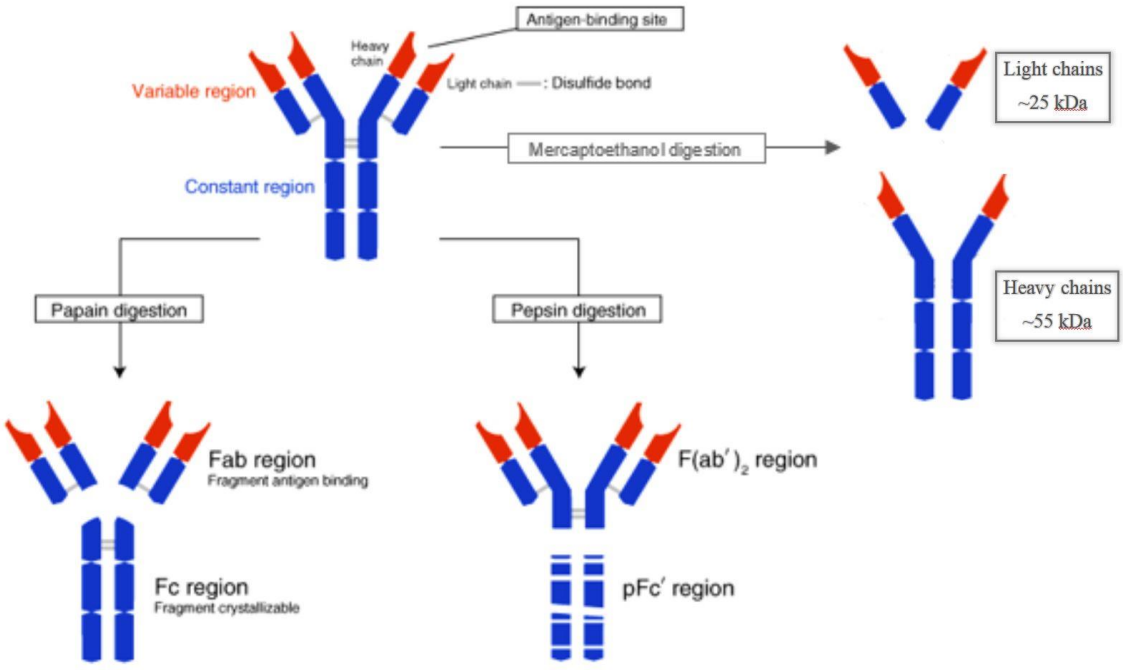

Figure 1. Structural components of an immunoglobulin molecule. Image adapted from: MBL Life Sciences, Japan.

Later it was determined that the Fc region was responsible for antibodies' many biological functions by virtue of binding specific cellular receptors (FcRs) on immune effector cells, such as macrophages, monocytes, neutrophils, dendritic, natural killer and mast cells; or by direct complement activation via binding of C1q.

Digestion with pepsin, another protease, cleaves off the Fab region with the hinge region attached (the structure termed $F(ab')_2$) while breaking the Fc region into small fragments (Figure 1).

Treating an antibody with mercaptoethanol, a reagent that breaks disulphide bonds, separate an antibody into four chains, two smaller ones of ~25 kDa consequently termed light chains and two larger ones of ~55 kDa termed heavy chains (Figure 1). Each immunoglobulin molecule contains one of the two types of light chains, κ or λ. The ratio of λ to κ chains varies between species, with 60% of total human immunoglobulins containing the former.[18]

Based upon the structure of the Fc region, immunoglobulins can be categorised into five classes or isotypes, including IgG, IgM, IgD, IgE, and IgA (Figure 2).[18]

Upon activation, B cells secrete IgM and IgD antibodies. However, as they proliferate under the influence of surrounding cytokines, B cells undergo class-switching to IgG, IgA or IgE without changing their antigenic specificity. The activating antigen determines the immunoglobulin class-switched isotype, while each isotype determines how the antigen will be eliminated and to which tissues the antibodies will be delivered.

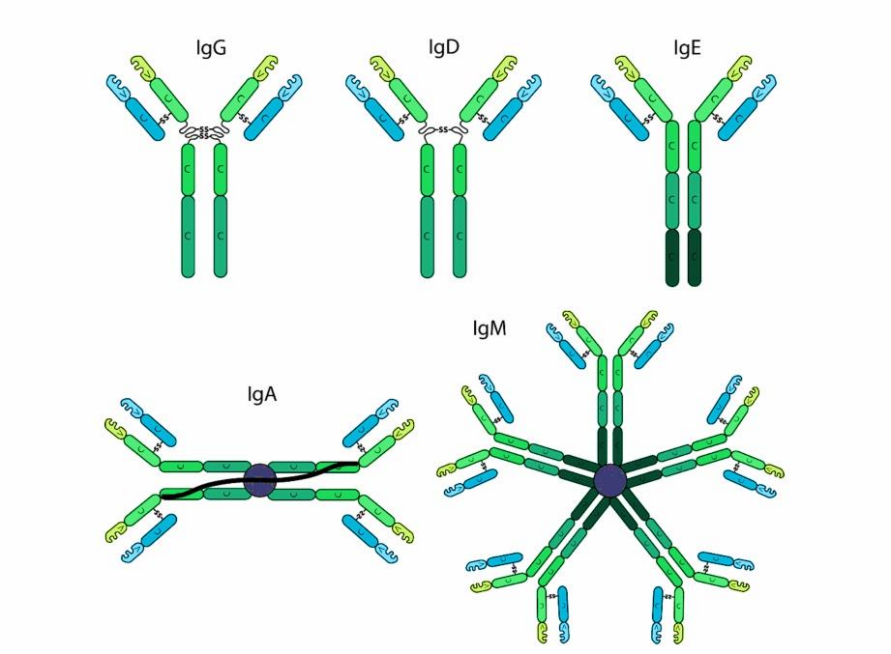

Figure 2. Five major classes of secreted antibodies. The polymeric IgM and IgA molecules contain a polypeptide known as the J chain (grey circle). Image source: SYnAbs, Belgium.

Although secreted IgD have been shown to be increased in some autoimmune conditions, such as rheumatoid arthritis, systemic lupus erythematosus, Sjögren's Syndrome and autoimmune thyroiditis, they constitute less than 1% of all secreted immunoglobulins.[19, 20] IgE antibodies are highly specific in their role in allergic responses and protection against parasitic infections. Outside of those conditions, their level in serum is extremely low. For these reasons, only immunoglobulins of G, M, and A isotypes are usually considered in autoimmunity.

1.2.3. Antibody autoreactivity and development of autoimmunity.

B cells development is tightly regulated at several checkpoints to control those clones that can react with self-antigens. Any self-reactive B cells can be removed from the repertoire through the mechanisms of deletion, energy, or receptor editing. However, some autoreactive B cells escape these regulatory checkpoints, and, if activated by a self-antigen, the production of autoantibodies may ensue.

Autoantibodies are increasingly recognised as the hallmark of many systemic autoimmune diseases, including systemic lupus erythematosus, rheumatoid arthritis, multiple sclerosis, autoimmune hepatitis, type 1 diabetes and many others.[21] While some disorders are characterised by the presence of one or a few autoantibodies, for example, anti-rheumatoid factor and anti-citrullinated protein antibodies in rheumatoid arthritis,[22] others, like systemic lupus erythematosus, are associated with more than 100 different autoantibodies.[23]

It should be mentioned that the presence of autoantibodies does not necessitate the development of autoimmunity. There is evidence to suggest that IgM autoantibodies are absolutely necessary for the maintenance of tissue homeostasis in healthy individuals.[24] In this role, they recognise self-antigens that are presented on apoptotic cells or senescent red blood cells and thus participate in the removal of apoptotic debris.[24] Additionality, even autoantibodies that are associated with a disease can be present in clinically healthy individuals. For example, rheumatoid factor antibodies are produced by patients with rheumatoid arthritis and Sjögren's Syndrome, as well

as healthy adults. Some evidence suggests that healthy and disease-associated autoantibodies might have structural differences causing the autoantibodies in healthy individuals to have less binding affinity to the target proteins.[25] Additionally, the appearance of autoantibodies might precede the development of a disease. In a retrospective study of patients with primary Sjögren's Syndrome, anti-rheumatoid factor antibodies were shown to appear as early as eighteen years before the clinical symptoms' onset.[26]

1.3. Autoantibodies in inclusion body myositis.

1.3.1. Humoral immunity in IBM.

Early investigations into the composition of immune cells that infiltrate IBM muscle found a high proportion of T-cells while detecting only minor numbers of B-cells.[27] However, when Greenberg *et al.* performed a microarray analysis of an IBM muscle in 2005, they found that nearly 60% of highly upregulated transcripts belonged to the immunoglobulin genes.[28] The group hypothesised that the immunoglobulins might have been produced by fully differentiated plasma cells that have lost the typical CD19 and CD20 B cell receptors and thus could not be detected in the previous studies. Indeed, using a specific plasma cell marker, CD138, Greenberg *et al.* were able to demonstrate a dense infiltration of plasma cells localised to the connective tissue encasing each myofiber.[28]

Following on, Bradshaw *et al.* carried out a comparison of immunoglobulin mRNA transcripts between IBM patients and healthy controls.[29] They found that the very few mature B cells present in the healthy control blood samples produced IgM only while most of the IBM plasma cells were class-switched from IgM to IgG or IgA.[29] This result suggested that IBM B cells were activated via the T-cell-dependent activation pathway by one or many self-antigens.[29] Sequencing of the immunoglobulin genes revealed that 85% of the myopathy samples (consisting of IBM, PM, and DM) contained clonally expanded B cells.[30] The clonal variants belonged to up to six different but related groups, and the same clonal groups were found in adjacent sections

of the same patient's muscle tissue.[30] In contradiction to the classic T-dependent B cell activation model, these findings strongly suggested that the clonal expansion took place within the muscle rather than in a spleen or a peripheral lymph node.[30, 31]

Further evidence of the antigen-driven humoral response came from functional studies that demonstrated strong binding of hemagglutinin-tagged recombinant IgG derived from a single IBM plasma cell to an intracellular self-antigen that was present in a skeletal muscle cell line.[32] The binding was also observed while incubating murine muscle tissue with human IgG derived from IBM patients' but not from healthy sera.[32] These experiments provided further evidence of serum circulating antibodies directed against one or many self-antigens in the IBM muscle tissue.

1.3.2. Anti-cN1A antibodies identification.

Western blot analysis of skeletal muscle lysates from patients clinically diagnosed with idiopathic inflammatory myopathies led Salajegheh *et al.* to identify a 43 kDa self-antigen present in 52% of IBM samples but not in DM, PM, myasthenia gravis or healthy controls.[33]

Two years later, the 43 kDa protein targeted by IBM autoantibodies was identified by two independent groups as cytosolic 5'-nucleotidase 1A (commonly abbreviated cN1A or NT5c1A). Larman *et al.* performed gel separation and mass spectrometry analysis on the IBM patients' muscle lysates.[34] By focusing on proteins between 40 and 48 kDa in size, the group identified seven potential candidates. A library of T7 phage transcripts containing 36-residue peptides spanning all the open reading frames in a human genome was created and screened using IBM and normal sera. Peptide-antibody complexes were precipitated and compared for the association with IBM. By combining the results of the mass spectrometry and phage precipitation experiments, cN1A protein was identified as the 43 kDa self-antigen with high confidence.

Simultaneously, Pluk *et al.*[35] used immunoaffinity purification to precipitate the protein of interest, which they termed Mup44 (Muscle protein with a molecular weight of 44,000 Da). They purified endogenous IgG from two IBM patients and a pool of healthy controls. Purified IgG

was covalently coupled to agarose beads that were subsequently used to precipitate Mup44 from human muscle lysate precleared from endogenous IgG. The precipitated protein was analysed by mass spectrometry and identified as cN1A.

1.3.3. Reactive epitopes.

Having identified the self-antigen as cN1A, both groups proceeded to establish which specific sites or epitopes of the protein are responsible for its interaction with the antibodies. Upon screening a phage library containing 36-residue overlapping peptides, Larman *et al.* identified three cN1A peptides that were present in reactive patients.[34] The immunodominant epitope near the N-terminus consisted of amino acids in positions 30 to 94 defined by two overlapping peptides 30-65 and 59-94 (Figure 3). The two other reactive epitopes occupied positions 204-239 and 334-368. Pluk *et al.* used ninety synthetic overlapping peptides to challenge cN1A-positive sera.[35] They also identified three reactive peptides comprising amino acids 25-50 (confirmed an immunodominant epitope), 221-243, and 341-368. Interestingly, the peptide occupying residues 59-94 identified by Larman et al.[34] was not confirmed reactive by Pluk *et al.*[35] Further experimentation is required to investigate this fourth putative epitope.

A later study probed 283 IBM patients' sera with the 23-amino acid peptides identified by Pluk *et al.*[35]: 59% of the reactive sera recognised one epitope only, while 25% recognised two and 15% recognised all three epitopes.[36]

```
1-60    MEPGQPREPQEPREPGPGAETAAAPVWEEAKIFYDNLAPKKKPKSPKPQNAVTIAVSSRA
61-120  LFRMDEEQQIYTEQGVEEYVRYQLEHENEPFSPGPAFPFVKALEAVNRRLRELYPDSEDV
121-180 FDIVLMTNNHAQVGVRLINSINHYDLFIERFCMTGGNSPICYLKAYHTNLYLSADAEKVR
181-240 EAIDEGIAAATIFSPSRDVVVSQSQLRVAFDGDAVLFSDESERIVKAHGLDRFFEHEKAH
241-300 ENKPLAQGPLKGFLEALGRLQKKFYSKGLRLECPIRTYLVTARSAASSGARALKTLRSWG
301-360 LETDEALFLAGAPKGPLLEKIRPHIFFDDQMFHVAGAQEMGTVAAHVPYGVAQTPRRTAP
361-368 AKQAPSAQ
```

Figure 3. Amino acid sequence of cytosolic 5'-nucleotidase 1A (cN1A). Coloured amino acids represent putative reactive epitopes targeted by anti-cN1A antibodies.

1.3.4. Cytosolic 5'-nucleotidase 1A.

The seven members of the 5'-nucleotidase enzyme family dephosphorylate nucleoside monophosphates into their constituent nucleosides and inorganic phosphates.[37] While some 5'-nucleotidase enzymes are ubiquitously expressed, cytosolic 5'-nucleotidase 1A expression is predominant in cardiac and skeletal muscles (Figure 4).

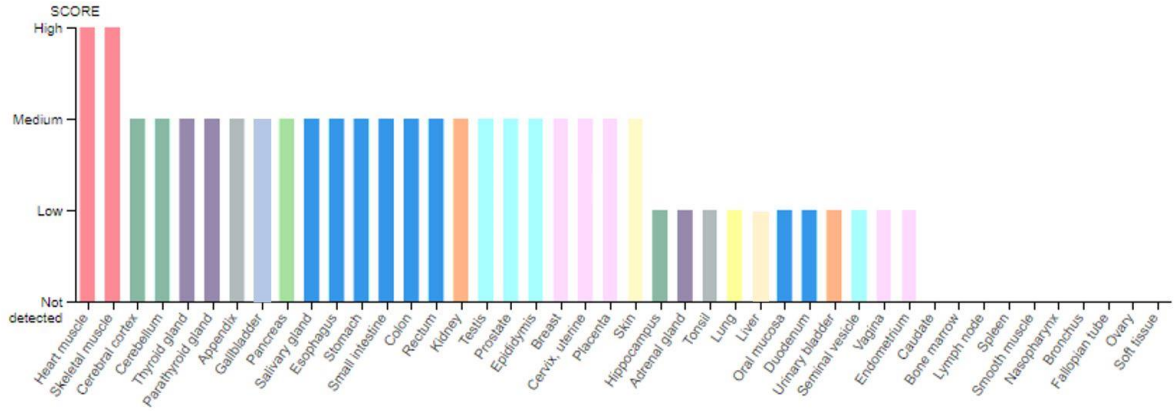

Figure 4. Cytosolic 5'-nucleotidase 1A expression in human tissues. The highest expression is observed in heart and skeletal muscles. Source: NCBI.

Cytosolic 5'-nucleotidase 1A has high specific activity with adenosine monophosphate (AMP) at millimolar concentrations.[38] By regulating pools of AMP, cN1A indirectly controls the "energy-sensing" AMP-activated protein kinase (AMPK) phosphorylation (Figure 5). The evidence for this relationship comes from the observation of a significant increase in phosphorylated AMPK levels during skeletal muscle stimulation of cN1A knockout mice.[39] In its role as an energy regulator, AMPK phosphorylates a large number of downstream enzymes resulting in inhibition of anabolic pathways and activation of catabolic pathways.[40]

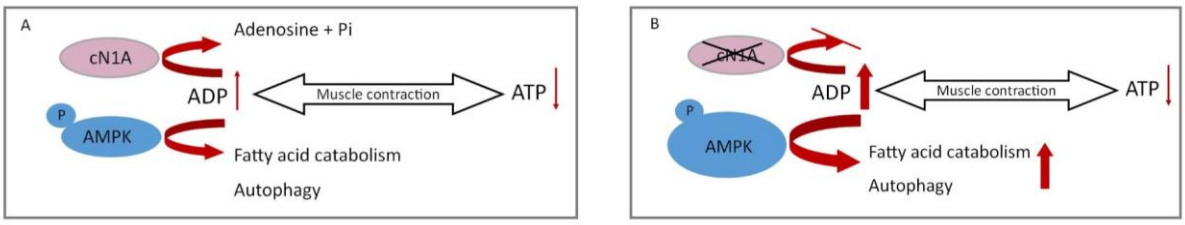

Figure 5. Regulation of cellular metabolism by cytosolic 5'-nucleotidase 1A and AMP-activated protein kinase. A. Healthy state: cN1A activity indirectly reduces activation of catabolic and autophagic regulators. B. Anti-cN1A-positive muscle: increased AMPK phosphorylation leads to upregulation of catabolic and autophagic regulators.

1.3.5. Anti-cN1A antibody pathogenicity.

Due to its prominent role in cellular metabolism, it is hypothesised that anti-cN1A antibody-binding could affect cN1A expression levels leading to an increase in catabolic processes and muscle degeneration. The most compelling evidence that this mechanism might be causing wasting of IBM muscles comes from a study assessing changes in protein expression levels *in vitro* and *in vivo* via supplementation of cells or passive immunisation of mice with anti-cN1A IgG from IBM patients.[41] The group observed a significant increase in sarcoplasmic aggregation of autophagy-related proteins p62/SQSTM1, a ubiquitin-binding adapter protein, and LC3, a microtubule-associated protein, both of which are pathological hallmarks of IBM muscle.[41] A simultaneous decrease in cN1A expression was also observed leading the authors to conclude that anti-cN1A antibodies may play a role in IBM pathogenicity.

1.3.6. Clinicopathological features of seropositive patients.

A small number of studies compared cohorts of IBM patients based on their anti-cN1A serology.[6, 34, 42-45] Upon evaluation of upper and lower muscle strength in a group of 25 IBM patients, Goyal *et al.* found seropositive patients to have a more severe motor weakness, more difficulty getting up from a standard chair and a higher chance of requiring a walker or a wheelchair for mobility.[6] Increased requirement for mobility assistance was confirmed in a cohort of 188 anti-cN1A seropositive patients.[43]

Seropositive IBM patients present with higher rates of dysphagia, facial muscle weakness and lower respiratory function as defined by lower forced vital capacity.[6] As a consequence, such patients' survival is on average 6.6 years shorter with an increased chance of dying from a respiratory disease than the seronegative group.[43]

No statistically significant correlation has been observed with anti-cN1A seropositivity to the presence of other antibodies (ANA, anti-Ro, anti-La) or diagnosis of other autoimmune diseases

(although, in one study 2 out of 33 anti-cN1A positive patients also had Sjögren's Syndrome and 2 had psoriasis).[34, 43]

Despite the significantly lower prevalence of IBM among females (38% compared to 61% in males),[11] one small study found an increased likelihood (83%) of a female patient to be anti-cN1A positive.[6] However, this association could not be confirmed in larger cohorts.[43-45]

Interestingly, one study found that muscle biopsy from seropositive patients was significantly less likely to contain rimmed vacuoles – an IBM diagnostic feature (62% vs 83%).[45] The authors speculate that increased anti-cN1A reactivity against the rimmed vacuoles could be the causative factor.[45] Subsequently, in cases where rimmed vacuoles are absent, the presence of anti-cN1A antibodies could help distinguish IBM from DM or PM.

No significant correlation was found between anti-cN1A positivity and patients' age, race, duration of symptoms, the strength of the weakest finger flexor and the strength of the weakest knee extensor.[6, 34, 42-44]

1.3.7. Anti-cN1A detection methods – enzyme-linked immunosorbent assay.

Since the identification of anti-cN1A antibodies, various assays have been developed for their detection in IBM patients' sera or muscle tissues. Some of the more commonly used detection methods are immunoblotting (otherwise known as Western blotting) with human or mouse muscle extracts[34, 35, 42] or cN1A-expressing human embryonic kidney 293 cell lysates,[6, 45] dot blot assay,[34] immunoprecipitation,[34, 35] and enzyme-linked immunosorbent assay (ELISA) with either full-length recombinant cN1A protein[4, 6, 42, 44, 46] or cN1A-derived synthetic peptides.[36, 42]

The specificity and sensitivity achieved by various diagnostic methods are summarised in Table 1. Here, the sensitivity describes the percentage of clinically-diagnosed IBM patients who are positive for anti-cN1A antibodies while the specificity refers to the proportion of seropositive patients who carry IBM diagnosis.

Table 1. Anti-cN1A antibodies detection methods presented in order of publication date from oldest to newest.

Reference	Method of detection	Cohort size	Sensitivity	Specificity
Salajegheh, 2011[33]	Immunoblot with muscle lysate	25	52	100
Pluk, 2013[35]	Immunoblot with muscle lysate	56	60	89
Larman, 2013[34]	Dot blot against 36-mer peptides	47	70	92
Greenberg, 2014[42]	ELISA against full protein (IgG)	50	51	94
Greenberg, 2014[42]	ELISA against full protein (combined IgG/IgA/IgM)	50	76	91
Herbert, 2016[36]	ELISA against 23-mer peptides	238	37	96
Kramp, 2016[4]	ELISA against full-length cN1A	17	35.5-39.2	96
Lloyd, 2016[45]	Immunoblot with HEK 293 lysate	117	61	87
Goyal, 2016[6]	Immunoblot with HEK 293 cell lysate	25	72	NA
Lilleker, 2017[43]	ELISA against 23-mer peptides	311	33	NA
Muro, 2017[46]	ELISA against full protein	10	80	89
Tawara, 2017[41]	COS7 cell-based assay (in-house)	67	36	92
Felice, 2018[44]	ELISA against full-protein	40	50	NA

Upon recognition of anti-cN1A antibodies as a useful diagnostic tool for IBM, a need arose to develop a standardised method that could be applied across diagnostic laboratories. Thus, a standardised ELISA for the detection of serum anti-cN1A antibodies of the IgG isotype was developed in 2016.[4] The assay will be discussed in detail later in this thesis. Despite the standardisation of the ELISA protocol, the range of the normal values is determined independently by each laboratory. In Kramp *et al.* study, the normal range was set as the mean optical density for the healthy controls cohort plus three standard deviations.[4] Caution is, therefore, required in interpreting ELISA results as the stringency of the normal range cut-off values may vary.[4, 44]

To determine the reproducibility and diagnostic value of the newly developed ELISA, the assay was used by two independent laboratories to test sera of patients diagnosed with IBM, other myopathies and unrelated autoimmune diseases as well as healthy controls. The sensitivity of the assay was independently determined to be 35.5% and 39.2% (reaching 47.1% in a group of patients with definite IBM) while the specificity was 96.1% and 96.5%.[4] Patients' sera were also tested by other established assays, namely ELISA based on three previously identified reactive epitopes[36] and the immunoprecipitation assay. The results were found to be highly correlated

between all tests. Notably, upon pooling data from various studies, anti-IgG only ELISA against cN1A peptides appears to be less sensitive (35%) than ELISA against the full-length protein (51%) possibly due to the reactivity of some polyclonal antibodies from a single patient to more than one cN1A epitope (Table 1 and section 1.3.3).

While the first ELISA was developed to test only for IgG isotype, it was later modified with the use of secondary antibodies against IgA, IgM and IgG isotypes.[42] Greenberg *et al.* found that including IgM and IgA isotypes increased ELISA sensitivity to 76%.[42]

The benefit of a standardised ELISA assay is that it can be applied across laboratories with highly reproducible results while being quicker and less laborious than other detection methods available. Another advantage is that ELISA lends itself well to high-throughput applications where multiple samples can be tested simultaneously. One of the main limitations of the assay is that upon coating of the wells with the antigen, some of the reactive epitopes might become masked. Thus, the antibody concentration value obtained by the ELISA could potentially be lower than the true serum concentration.

The specificity of anti-cN1A antibodies for IBM is over 87% supporting their value as a valuable diagnostic tool for the condition (Table 1). However, it is noteworthy that anti-cN1A antibodies have been detected in patients with other myopathies, autoimmune diseases, and in healthy population, albeit a lot less frequently than in IBM (Table 2).

Table 2. Prevalence of the anti-cN1A antibodies in various diseases.

Disease Diagnosis	Anti-cN1A reactivity (%)
Inclusion Body Myositis	33%-80%[43, 46, 47]
Polymyositis	4%-4.8%[36,45]
Dermatomyositis	15%[45]
Sjögren's syndrome	0%[4, 47], 6%[34], 12%[48], 23%[45], 36%[36]
Systemic lupus erythematosus	6,1%[4], 10%[48], 14%[45, 47], 20%[36]
Psoriasis	6%[34]
Scleroderma	2%,[36] 10%[4]
Rheumatoid arthritis	0%,[47] 2%,[36] 5%[4]
Multiple sclerosis	5%[36]
Type 1 diabetes	0%[36]
Healthy controls	3%[36], 4.8%[45]

Higher prevalence of anti-cN1A antibodies in patients with IBM comparing to polymyositis patients suggests their utility in distinguishing those two clinically similar conditions. However, the diagnosis of IBM cannot be solely based on a patient's seropositivity status since up to 5% of polymyositis patients also develop anti-cN1A antibodies.[36, 45] It has not been determined whether anti-cN1A-positive polymyositis patients go on to be diagnosed with IBM later in the disease progression.

Dermatomyositis patients test positive for anti-cN1A antibodies in up to 15% of cases,[45] while patients with Sjögren's Syndrome and systemic lupus erythematosus can be seropositive in up to 36% and up to 20% of cases respectively.[36] Interestingly, DM, systemic lupus erythematosus and Sjögren's Syndrome patients positive for anti-cN1A do not have a defined clinical phenotype and appear to be indistinguishable from seronegative patients.[45] An increased incidence of anti-cN1A antibodies in these patients is not diagnostically significant since the conditions are clinically distinct from IBM. However, it might be evidential of common underlying autoimmune mechanisms or genetic background for these diseases that are yet to be uncovered.

1.4. Therapeutic targeting of anti-cN1A antibodies with DNA aptamers.

Due to the anti-cN1A diagnostic significance and their potential involvement in IBM pathogenicity, these autoantibodies can be a promising target for therapeutic aptamer development. Aptamers are single-stranded oligo(deoxy)nucleotide (DNA or RNA) constructs of 20-80 bases in length that are capable of binding a selected target with high affinity and specificity due to their unique three-dimensional structure (Figure 6).[49, 50] The conformation

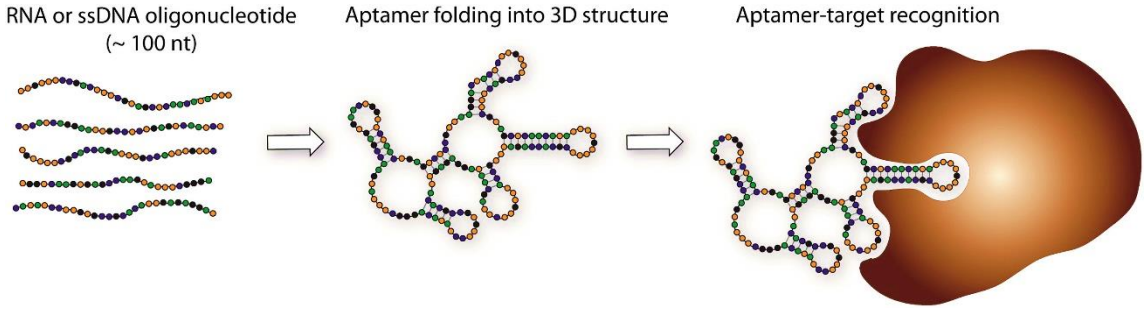

Figure 6. Schematic representation of an aptamer–target interaction.

depends primarily on the aptamer sequence but also the environmental conditions (e.g. temperature, pH, buffer composition etc.).[51] Since their discovery more than 25 years ago,[52-54] aptamers have been designed for a plethora of targets, such as small molecules,[55] proteins and peptides,[56] viruses,[57] bacteria and living cells.[58] Due to their specific binding ability, aptamers can be likened to monoclonal antibodies, but there are some important factors favouring the use of aptamers in bioanalytical and therapeutic applications.[59] One significant functional difference is that aptamers denatured under certain conditions such as high temperatures can refold into their original tertiary structures when the conditions return to favourable. Denaturation of antibodies, like other proteins, cannot be reversed. Additionally, aptamers (i) have reduced immunogenicity and toxicity, (ii) can be synthesised following an established chemical procedure minimising batch-to-batch variations, (iii) can be chemically modified to increase resistance to nucleases *in vivo* or to introduce reporter probes (fluorophores) for visualisation in a site-specific manner.[49] In their interactions with proteins, aptamers bind to a specific domain

thus potentially inhibiting the associated protein function, e.g. interaction of an autoantibody with a self-antigen.[60]

1.4.1. SELEX aptamer selection.

To achieve high-affinity binding, a large pool of randomly generated nucleic acid sequences undergo a process of repetitive *in vitro* selection, termed SELEX (systematic evolution of ligands by exponential enrichment).[53] Both DNA and RNA sequences can be used for SELEX depending on the target application. Historically, RNA was preferred due to its ability to form more diverse three-dimensional structures.[61] However, working with RNA is tedious as it can be easily degraded by ubiquitous RNAses, high temperatures etc. Thus, much of the current SELEX research is conducted with single-stranded DNA which is more robust while still able to fold into intricate functional motifs.[62]

SELEX process begins with the generation of a chemically synthesised library containing a random sequence of 20-40 nucleotides flanked by constant primer-binding sites.[63] In the case of RNA aptamer generation, the starting RNA library is first transcribed into DNA that then undergoes selection like DNA aptamers.

The SELEX cycle entails incubation of the nucleotide library with the target molecule, washing the unbound aptamers away, recovering the bound aptamer-protein constructs and amplifying the selected sequences by PCR in case of DNA or RT-PCR in case of RNA (Figure 7).[61] The process is repeated 5-16 cycles to sufficiently enrich the aptamer population for high affinity and

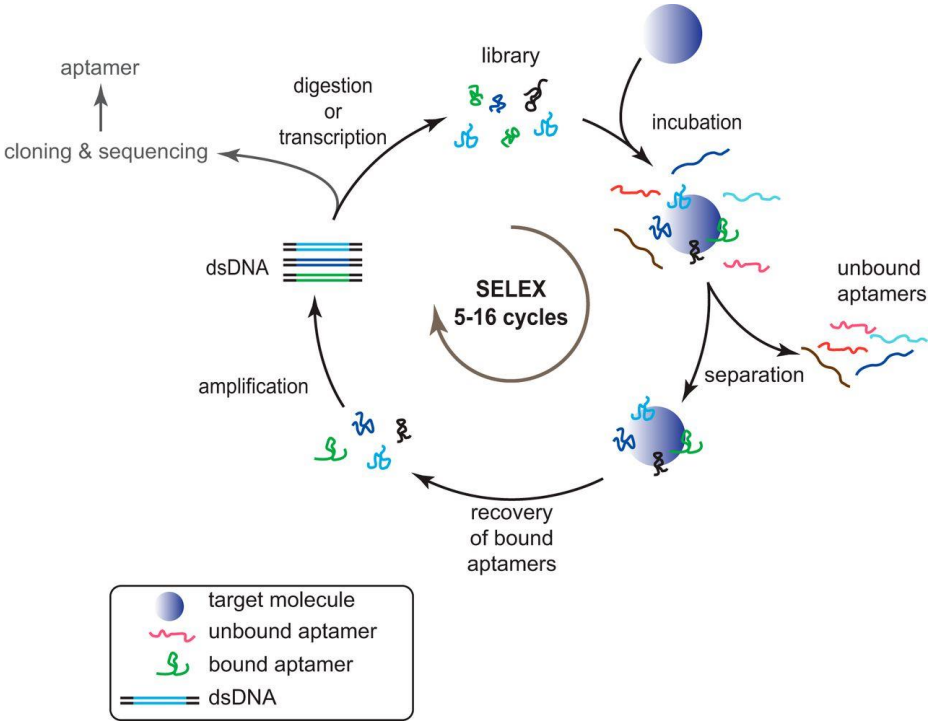

Figure 7. Schematic illustration of an in vitro SELEX selection process. Image source: Darmostuk et al.

specificity. Potential aptamers recovered from SELEX are sequenced and their binding kinetics evaluated by various methods.

Since its development more than 20 years ago, SELEX has undergone countless modifications.[61] Here, it is worth mentioning that in line with changes to the actual *in vitro* selection process, multiple *in silico* approaches have also been developed that have become an integral part of almost all SELEX experiments. Numerous computational programs can be used for the prediction of aptamer tertiary structure, its target interactions and thermodynamic characteristics.[61] While computational approaches can reduce the cost and time of high-affinity aptamer generation, they can only be used in combination with conventional SELEX since they require prior knowledge of the target sequence and the selected aptamer sequences which can then be modified *in silico* to increase their binding affinity to the target.[61]

1.4.2. Aptamers against immunoglobulin targets.

Development of aptamers against autoantibodies associated with various autoimmune diseases has been given much attention in the last two decades with promising results. Doudna *et al.* identified a short RNA sequence using selection against a mouse monoclonal antibody, MA20, that recognises human insulin receptor.[50] Patients with severe insulin resistance often develop autoantibodies that recognise the same epitope as MA20. Indeed, the developed anti-MA20 RNA aptamer showed efficacy in binding anti-insulin receptor antibodies in human patient sera thus blocking the autoantibody-receptor interaction.[50] This finding, however, had limited therapeutic application since RNA transcripts have a short half-life in serum due to the presence of nucleases. This problem was overcome by the modification of the "decoy RNA", as it was originally termed, where all pyrimidine nucleotides (uracil and cytosine) were replaced with a 2'-amino group.[64] Inclusion of the 2'-amino group increased the RNA stability in serum by more than 10,000-fold while not affecting its ability to bind the insulin receptor on the surface of human lymphocytes.[64] Similarly, RNA pyrimidines can be substituted by a 2'-fluoro analogues to enhance an aptamer's nuclease resistance.[65] Effective RNA aptamers have since been designed against anti-DNA autoantibody G6-9 present in systemic lupus erythematosus patients,[66] and anti-acetylcholine receptor antibody Mab198 in myasthenia gravis.[67, 68]

Autoantibodies against various G-protein coupled receptors (beta1-, beta2-, alpha1-adrenoreceptors, anti-endothelin A receptor, ET_A-receptor etc.) have been implicated in the pathogenesis of a group of diseases, encompassing cardiomyopathies, hypertension, diabetes mellitus, Alzheimer's disease and others.[69] An exciting possibility would be to develop an aptamer-based therapeutic that could target the antibodies in all of these conditions. Interestingly, a DNA aptamer BC 007, initially developed against thrombin, showed efficacy in neutralising multiple anti-G-protein coupled receptor antibodies *in vitro* and *in vivo* in hypertensive rats.[69] Moreover, BC 007 appears to be specific for human G-coupled receptor autoantibodies while

having no efficacy with other autoantibody types and little to no efficacy with G-coupled receptor autoantibodies from other species (other than rats).[69] Due to its specificity and efficacy at low doses, BC 007 was entered into clinical trials as an autoimmune cardiomyopathy treatment, of which phase one was completed in 2018.[70] These cases present compelling evidence for autoantibody-neutralising aptamers' therapeutic potential.

1.5. Project Outline.

This research project will investigate a selection of DNA aptamers that can target anti-cN1A antibodies to prevent their interaction with cN1A protein. In doing so, we hope to ameliorate IBM symptoms and halt the disease progression.

The first part of the project will encompass screening of the biobanked IBM sera with anti-cN1A ELISA. A single patient with high autoantibody titres will be selected for a repeat serum collection from which anti-cN1A antibodies will be purified.

In the second part of the project, the purified anti-cN1A antibodies will be utilised for the aptamer selection by a modified SELEX methodology. The first cycle of selection will be performed from the initial library of synthesised DNA fragments (aptamers) containing a 40-nucleotide randomised region flanked by the 5′ and 3′ constant regions serving as primer-binding sites. The selected aptamers that effectively conjugate with the antibodies' binding region will be isolated and employed as a library for the following selection cycle.

The efficacy of the aptamer neutralisation will be confirmed by an ELISA where the binding of purified anti-cN1A antibodies to cN1A protein in the absence of aptamers will be compared to their binding upon the addition of the selected aptamers at a range of concentrations.

The success of this project may lead to the discovery of a novel therapeutic for anti-cN1A-positive IBM patients. Moreover, the established methodology may be applied to other autoimmune conditions where antibodies have been demonstrated to play a pathogenic role.

CHAPTER 2. Materials and methods.

2.1. Patients and Controls.

Clinically diagnosed IBM patients were recruited through their primary clinician Prof Merrilee Needham (Fiona Stanley Hospital, Murdoch, WA) in accordance with the protocols approved by the Murdoch Human Experimentation Ethics Committee (approval # 2015/111). Blood samples were collected at the Institute for Immunology and Infectious Diseases within twelve months prior to the study. All samples were fractioned upon collection with the serum portion biobanked and stored at -80°C.

Pooled healthy sera were obtained from the Busselton Health Study Group (University of Western Australia, Perth, Western Australia).

2.2. Anti-cN1A enzyme-linked immunosorbent assay (ELISA).

N-terminal histidine-tagged cN1A protein (RefSeq NP_115915.1; Cat. No. P10011809; GenScript, New Jersey, United States) was diluted with 0.05 M carbonate-bicarbonate buffer (34.3 mM Na_2CO_3, 15.7 mM $NaHCO_3$, pH 9.6) to the final concentration of 10 μg/mL. To coat a Microtitre 96 well plate (Maxisorp, Nunc, Roskilde, Denmark), 50 μL of the protein per well was incubated for two hours at room temperature. After washing the plate three times with 500 μL PBST (2.7 mM KCl, 137 mM NaCl, 1.5 mM KH_2PO_4, 15.2 mM Na_2HPO_4, 0.1% Tween-20, pH 7.4) in the automatic plate washer (ELx405, BioTek), the wells were blocked with 250 μL blocking buffer (PBST pH 7.4, 5.0% skim milk powder) overnight at 4°C.

The following day the plate was brought to room temperature and washed as before. Patients' sera were diluted 1:1000 with blocking buffer, and 50 μL was added to each well, followed by a two-hour incubation at room temperature. Subsequently, wells were washed as before and incubated for two hours at room temperature with 100 μL goat anti-human horseradish peroxidase (HRP)-conjugated antibodies against IgG (Cat. No. 31410; Invitrogen, Rockford, IL, USA); IgA (Cat. No. 31417; Invitrogen, Rockford, IL, USA); IgM (Cat. No. 31415; Invitrogen,

Rockford, IL, USA) and IgG/M/A (Cat. No. 31418; Invitrogen, Rockford, IL, USA). Upon receipt, the antibodies were diluted 1:2 with glycerol (Univar), aliquoted into 100 or 500 µL volumes, and stored at -20°C. Prior to use, the aliquoted antibodies were thawed at room temperature and diluted with blocking buffer at 1:10,000 for IgG and IgG/M/A, 1:5,000 for IgA and 1:2,000 for IgM.

Thirty minutes prior to use, one tablet of TMB (3,3,5,5-tetramethylbenzidine) substrate solution (Cat. No. T5525-50TAB; Sigma-Aldrich) was added to 10 mL of 0.05 M phosphate-citrate buffer (0.05 M citric acid, 0.1 M Na_2HPO_4, pH 5.0) in a 15 mL test tube wrapped in aluminum foil and incubated on a tube rotator (MACSmix, Miltenyi Biotec) at room temperature to assist with the tablet dissolution. Immediately before use, 10 µL of 6% hydrogen peroxide was added to the TMB solution. 6% hydrogen peroxide was prepared from 30% solution (Cat. No. H1009, Sigma-Aldrich).

Finally, after washing the plate as before, bound antibodies were visualised by adding 100 µL of the TMB solution. The reaction was stopped after 10 minutes by the addition of 25 µL 2 M sulphuric acid (prepared from 100% sulphuric acid (Cat. No. 339741, Sigma-Aldrich). The absorbance was read at 450 nm by the multi-mode microplate reader (FLUOstar Omega, BMG LABTECH).

Every serum sample was tested in duplicate with each secondary antibody isotype. Each plate contained an internal positive control (a previously-tested positive sample), a healthy control (pooled healthy sera) and a blank (cN1A-coated well without sera).

Absorbance values obtained for all patients' sera samples were recorded as a fold change relative to healthy sera.

A reference seropositive range was previously determined by Bundell *et al.*[71] as the 99th percentile of the pooled healthy control (same pooled control as used in this project).

2.3. Magnetic bead purification of serum anti-cN1A antibodies.

90 mL of blood from a selected IBM patient was collected at the Institute for Immunology and Infectious Diseases collection centre into serum tubes with gel separators. The tubes were centrifuged (Allegra X-22R, Beckman Coulter) at 14,000 rotations per minute (RPM) for 10 minutes to fraction the blood. The serum was aspirated into 5 mL Falcon® round-bottom polystyrene tubes (Cat. No. 352054; Corning) and stored at 4°C.

The antibodies purification was performed using Dynabeads® magnetic beads for histidine-tagged isolation and pulldown (Cat. No. 10103D; Invitrogen, Vilnius, Lithuania) coated with N-terminal histidine-tagged cN1A protein (RefSeq NP_115915.1; Cat. No. P10011809; GenScript, New Jersey, United States). Protein conjugation to the beads was achieved by combining 152 µL of cN1A diluted in 1400 µL of binding/wash buffer (0.05 M NaH_2PO_4, 0.3 M NaCl, 0.02% Tween-20, pH 8.0) with 42 µL of stock beads. Following a five-minute incubation at room temperature on a tube rotator, the beads were washed four times by alternating rounds of resuspension in 300 µL of binding/wash buffer, a two-minute incubation on the EasyEights EasySep magnet (Cat. No. 18103; Stemcell Technologies) and supernatant aspiration with a pipette. After the third wash, the beads were resuspended in 300 µL binding/wash buffer and evenly split into two 1.5 mL Eppendorf tubes before placing on the magnet for two minutes and aspirating the supernatant. 1.5 mL of undiluted serum was added to each Eppendorf tube, and the coated beads were incubated with the serum on a tube rotator (MACSmix, Miltenyi Biotec) at room temperature for two hours. During incubation, serum anti-cN1A antibodies were captured by the bead-immobilised cN1A protein. The beads were washed as previously described four times with 500 µL HEPES (4-(2-hydroxyethyl)-1-piperazineethanesulfonic acid) buffer (pH 7.2) containing 0.06% Tween-20. Bound antibodies were eluted with 190 µL Pierce® gentle antigen/antibody elution buffer (Cat. No. 21027; Thermo Scientific, Rockford, IL, USA) by incubating the beads with the buffer for ten minutes at room temperature on a shaker plate. The

buffer facilitated disassociation of the antibodies from cN1A protein while the protein remained conjugated to the beads for further use.

Following a two-minute incubation on the magnet, the supernatant containing purified antibodies was collected. The elution was then repeated two more times. Following the last elution round, beads were washed three times with 500 µL HEPES buffer.

Between experiments, coated beads were stored in 500 µL HEPES buffer at 4°C.

Each 1.5 mL of serum underwent a minimum of three rounds of depletion.

Purified antibodies were then dialysed to replace the elution buffer with PBS (2.7 mM KCl, 137 mM NaCl, 1.5 mM KH_2PO_4, 15.2 mM Na2HPO4, pH 7.4) for long-term storage. For dialysis, 3.5 – 4 mL of the eluted antibodies were loaded into a Slide-A-Lyzer™ dialysis cassettes (3.5K molecular weight cut off, Cat. No. 66330; Thermo Scientific, Rockford, IL, USA) and floated in 2 L of PBS overnight at 4°C. The following day, 9 mL of antibody/PBS suspension was pipetted from each dialysis cassette into 15 mL test tubes and stored at 4°C or immediately concentrated. To concentrate the antibody-containing solution, 15 mL was loaded into an Amicon® Ultra-15 centrifugal filter device (10K molecular weight cutoff, Cat. No. UFC901024; Merck Millipore) and centrifuged (Allegra X-22R, Beckman Coulter) at 4000 x g relative centrifugal force (RCF) for 15 minutes at 4°C. Post centrifugation, each collection tube contained between 550 and 950 µL of anti-cN1A in PBS. Concentrated antibodies were stored at 4°C. A fraction of purified antibodies in excess to the SELEX requirement was combined with equal volume of glycerol and stored at -80°C.

2.3.1. Purified anti-cN1A quantification by bicinchoninic acid (BCA) protein assay.

The concentration of the purified anti-cN1A antibodies in the solution was quantified using Pierce® bicinchoninic acid (BCA) protein assay kit (Cat. No. 23225; Thermo Scientific, Rockford, IL, USA). The assay was performed according to the manufacturer's instructions for a microplate procedure. Briefly, 1 mL ampule containing 2 mg/mL bovine serum albumin (BSA)

was diluted in PBS (2.7 mM KCl, 137 mM NaCl, 1.5 mM KH_2PO_4, 15.2 mM Na2HPO4, pH 7.4) to prepare a set of protein standards with the final protein concentrations of 2000, 1500, 1000, 750, 500, 250, 125, 25 and 0 µg/mL.

Purified antibodies were diluted in PBS at the ratios of 1:2, 1:7, 1:49 and 1:343.

A working reagent was prepared by combining 5,000 µL of Reagent A with 100 µL of Reagent B. All solutions were thoroughly vortexed before adding 25 µL of each standard and sample dilution to a Microtitre 96 well plate. 200 µL of the working reagent was then added to each well and mixed with a pipette. The plate was covered and incubated at 37°C for 30 minutes. Following the incubation, the plate was cooled to room temperature, and the absorbance was read at 570 nm wavelength by the multi-mode microplate reader (FLUOstar Omega, BMG LABTECH).

2.4.2. Protein sodium dodecyl sulphate polyacrylamide gel electrophoresis (SDS-PAGE).

To hand cast one gradient gel, 8 mL of resolving polyacrylamide gel solution was prepared by combining 2 mL of 40% SureCast acrylamide solution (Cat. No. HC2040; Life Technologies, Carlsbad, CA, USA), 2 mL of resolving buffer (0.38 M Trizma base, pH 8.8), 80 µL of 10% SureCast ammonium persulfate and 3.9 mL of deionised water. 10% ammonium persulfate was prepared by dissolving 100 mg ammonium persulfate (Cat. No. HC2005; Life Technologies, Carlsbad, CA, USA) in 1 mL of MilliQ water and stored as 90 µL aliquots at -20°C. 8 µL of SureCast TEMED (Cat. No. HC2006; Life Technologies, Carlsbad, CA, USA) was added to the solution immediately before pouring into a 1 mm-thick Mini-Protean casting cassette (Bio-Rad). A thin layer of 100% isopropanol was pipetted on top of the gel to flatten the top edge and protect the gel from oxidation. The gel was set for 20 minutes.

Meanwhile, 4% polyacrylamide stacking gel solution was prepared by combining 0.3 mL of 40% SureCast acrylamide solution, 0.75 mL of 1 M Tris-HCl buffer (pH 6.8) prepared from UltraPure

1 M Tris-HCI buffer, pH 7.5 (Cat. No. 15567027; Invitrogen, Rockford, IL, USA), 30 µL of 10% SureCast ammonium persulfate and 1.92 mL deionised water.

Once the resolving gel was set, the isopropanol layer was removed with Kimwipes (Kimtech), and the gel edge was rinsed with deionised water. 3 µL of TEMED was then added to the stacking solution, and the solution was poured on top of the resolving gel. The gel was fitted with a Mini-Protean 1.0 mm 10-well comb (Bio-Rad) and set for 15 minutes.

Reduced and non-reduced protein samples were prepared. For non-reduced preparation, samples were combined with equal volumes of loading buffer (4% SDS, 25 mM EDTA, 0.01% bromophenol blue, 20% glycerol, 125 mM Tris-HCl, pH 6.8). For reduced preparation, samples were combined as before with the addition of 0.35 mM dithiothreitol (DTT) and heated at 95°C for 10 minutes. Samples were kept at room temperature until loading.

Once set, the casting cassette was removed from its holder and inserted into a Mini-Protean tetra cell (Bio-Rad) opposite another gel or the buffer dam. The internal chamber was filled with running buffer (25 mM Trizma base, 191.8 mM glycine, 3.5 mM SDS, pH 8.3) while the cell was filled with the same buffer to the "2 Gels" mark (~ 500 mL total buffer volume). Wells were loaded with 8 µL of each sample or loading buffer diluted 1:1 with MilliQ water so that no empty wells remained. The electrophoresis was run at constant 90 volts for 1 hour 45 minutes until the loading dye travelled to the bottom edge of the gel. Once complete, the gel was removed from the cassette and stained for 10 minutes with Coomassie blue staining solution (0.001% Coomassie Brilliant Blue (Bio-Rad), 50% methanol, 10% glacial acetic acid) on a plate shaker. Subsequently, the gel was destained in 7% acetic acid solution overnight. The following day, the gel was imaged with Fusion FX (Vilber Lourmat) chemiluminescence detector.

2.4. Positive selection of aptamers against anti-cN1A binding sites.

Initial DNA library (Integrated DNA Technologies, Coralville, IA) was synthesised with a 40-nucleotide randomised region containing equal parts of A, T, G and C flanked by the 5′ constant

region *5′-GGA CAG GAC CAC ACC CAG CG-3′* and the 3′ constant region *5′-GGC TCC TGT GTG TCG CTT TGT-3′*. The library was diluted with PBS (2.7 mM KCl, 137 mM NaCl, 1.5 mM KH_2PO_4, 15.2 mM Na2HPO4, pH 7.4) to 1 mM and stored at 4°C.

100 nmol of the initial DNA library containing approximately 6 x 10^{16} unique sequences (Equation 1) was used in the first round of selection.

Equation 1. Sequence diversity of the DNA library.

Library diversity = (n)*(Avogadro's number), where n = moles of library used

Library diversity in round one = 100 x 10^{-9} mol x 6.022 x 10^{23} mol^{-1} = 6 x 10^{16} sequences

The library was added to 600 µL aptamer binding buffer (2.7 mM KCl, 137 mM NaCl, 1.5 mM KH_2PO_4, 15.2 mM Na_2HPO_4, 0.02% Tween-20, 2.5 mM $MgCl_2$, pH 7.4) in 1.5 mL Eppendorf tube and heated to 95°C for 10 minutes. As the solution cooled to room temperature, the oligonucleotides folded into their respective tertiary structures. Subsequently, 1 µL of anti-cN1A antibodies was added to the library, and the solution was incubated on a roller at room temperature for one hour during which time some of the aptamers bound to the antibodies (Figure 8, A).

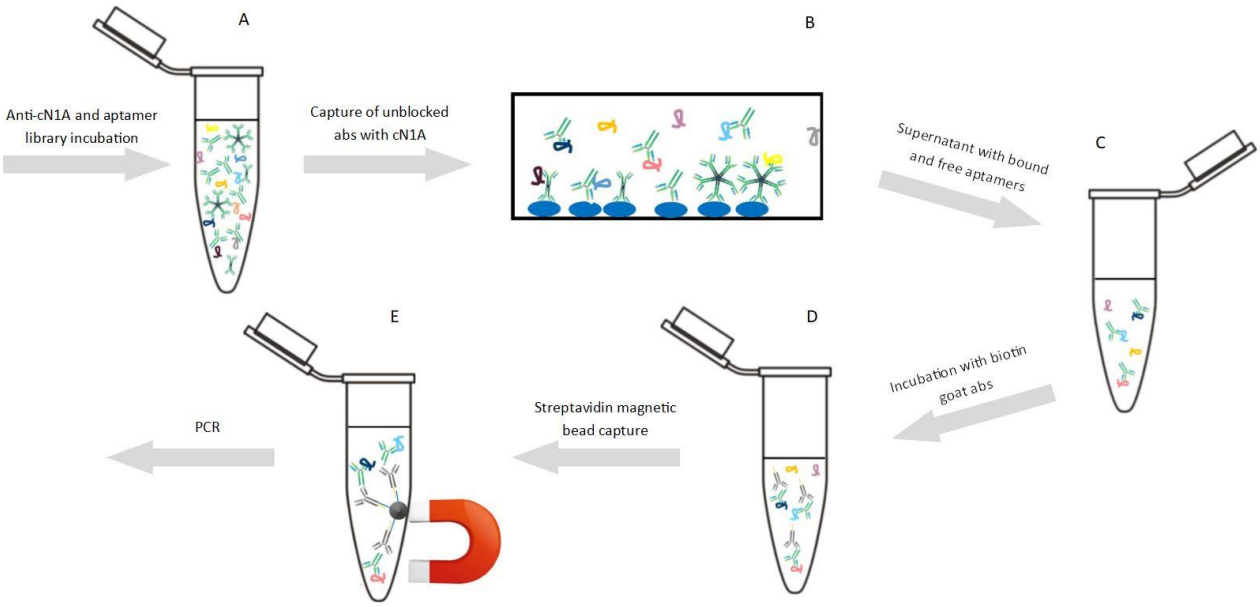

Figure 8. Schematic representation of the stages of positive selection of aptamers against anti-cN1A binding site.

To isolate specific antibody/aptamer complexes where the aptamer was interacting with the anti-cN1A binding site, the suspension was challenged with the immobilised cN1A protein (Figure 8, B). For this, Microtitre 96 well plates were coated with N-terminal histidine-tagged cN1A protein (RefSeq NP_115915.1; Cat. No. P1EF001; GenScript, New Jersey, USA) diluted with 0.05 M carbonate-bicarbonate buffer (34.3 mM Na_2CO_3, 15.7 mM $NaHCO_3$, pH 9.6) to the final concentration of 20 μg/mL as per the standard ELISA protocol (section 2.2).

Following the incubation, the aptamer/antibody solution was added to 9.4 mL PBST (2.7 mM KCl, 137 mM NaCl, 1.5 mM KH_2PO_4, 15.2 mM Na_2HPO_4, 0.1% Tween-20, pH 7.4) in a 15 mL conical tube and mixed inversion to achieve final antibody dilution of 1:10,000. For the separation, 50 μL of the solution was added to each cN1A-coated well. The plates were sealed and incubated at room temperature for two hours. During the incubation, the antibodies that were either not aptamer-bound or bound at a site that does not interfere with antibody/cN1A interaction were captured by the immobilised cN1A and cleared from the supernatant. The supernatant now containing the desired aptamers as well as unbound oligonucleotides was collected from each well and pooled into a 15 mL tube (Figure 8, C).

To isolate the antibody-bound and unbound aptamers, the supernatant was incubated with 0.5 μL biotin-conjugated goat anti-human IgG, IgM, IgA (H+L) secondary antibodies (Cat. No. A18851; Invitrogen, Rockford, IL, USA) on a tube rotator for one hour at room temperature (Figure 8, D).

Meanwhile, 5 μL of Dynabeads® M-280 streptavidin magnetic beads (Cat. No. 11205D; Invitrogen, Vilnius, Lithuania) were washed with 1 mL PBST and added to the secondary antibody/anti-cN1A/aptamer solution. The mix was placed on a tube rotator for a further 30 minutes to allow for the biotin-streptavidin interaction to occur. Following the incubation, the tube was placed on a magnet for 3 minutes, and the supernatant containing unbound aptamers was removed and discarded leaving only the desired binders attached to the beads (Figure 8, E).

The beads were then washed five times with 500 µL PBS. Each addition of PBS was followed by thorough vortexing and placing on a magnet for 3 minutes. Following the last washing cycle, the beads were resuspended in 100 µL of Tris-EDTA buffer, pH 8.0 (83% UltraPure 1 M Tris-HCI Buffer, pH 7.5 (Cat. No. 15567027; Invitrogen, Rockford, IL, USA), adjusted pH to 8.0 with 5M NaOH, 17% UltraPure 0.5M EDTA, pH 8.0 (Cat. No. 15575020; Invitrogen, Rockford, IL, USA)) and transferred into a 1.5 mL Eppendorf tube. The suspension was then heated to 95°C for 10 minutes to denature the proteins and elute the DNA. The mixture was cooled to room temperature and placed on a magnet for 3 minutes. The supernatant containing selected aptamers was removed into a clean 1.5 mL Eppendorf tube and stored at -20°C.

2.5. Polymerase chain reaction (PCR).

All PCR reactions were performed using Phusion high-fidelity PCR master mix with HF buffer (Cat. No. F531; Thermo Fisher Scientific, Vilnius, Lithuania) and UltraPure™ DNase/RNase-free distilled water (Cat. No. 10977015; Invitrogen, Rockford, IL, USA). Forward primer 5′-20T-iSp9-ACAAAGCGACACACAGGAGCC-3′ and reverse primer 5′-GGACAGGACCACACCCAGCG-3′ were synthesised by Integrated DNA Technologies, Coralville, IA, USA. Aptamer amplification was performed by a LifeTouch thermal cycler (Bioer Technology, Hangzhou, P.R. China) in 50 µL PCR reactions containing the reagents and volumes presented in Table 3. A positive control of 10 µM initial DNA library and a negative control containing no DNA template were included in each PCR run.

Table 3.Component volumes of a single 50 µL polymerase chain reaction for the amplification of the selected DNA aptamers.

Reagents	Volume per reaction (µL)
Phusion Master Mix	25.0
Forward primer (10 uM)	2.0
Reverse primer (10 uM)	2.0
UltraPure water	18.0
DNA template/UltraPure water	3.0
Total volume	50.0

The optimal cycling conditions were developed by T. Wang (unpublished) and are summarised in Table 4.

Table 4. Polymerase chain reaction program for the selected DNA aptamers amplification.

Cycle Step	Temperature (°C)	Time (sec)
1. Initial denaturation (polymerase activation)	98	30
2. Denaturation	95	30
3. Annealing	51.6	40
4. Extension	72	45
Repeat steps 2-4 for n cycles		

2.5.1. Initial amplification of the selected aptamers.

The aptamer library used in the first round of selection consists of randomly generated DNA sequences, hence every oligonucleotide copy is unique. Thus, it was necessary to perform an initial ten-cycle amplification to create additional copies of each sequence. From the second round of selection onward, the initial amplification was performed to increase the amount of the

DNA template available, subsequently increasing the final amount of each amplicon available for the following SELEX cycle.

For the initial amplification, 50 µL PCR reactions (Table 3) were set up in Axygen® 8-strip PCR tubes (Cat. No. PCR-0108-LP-C; Corning) and amplified using the standard PCR program (Table 4). The double-stranded product of amplification (excluding the controls) was pooled into one volume. 10 µL were retained and stored at -20°C as a selected library backup. The remaining fraction was used as a template for the analytical PCR.

2.5.2. Analytical aptamer amplification.

Analytical PCR was performed to identify the optimal number of amplification cycles that would yield the highest amount of product of the expected size without producing additional undesired by-product.

50 µL PCR reactions (Table 3) were prepared in single Axygen® PCR tubes (Cat. No. PCR-02D-A; Corning) to be amplified at varied number of cycles using the standard PCR program (Table 4). All reaction tubes were inserted into one thermocycler, the cycling was manually paused after the extension phase of the relevant cycle, and the corresponding reaction tube was removed. A positive control was amplified for 10 cycles, and a negative control was amplified for the maximum number of cycles in the PCR run.

Following the amplification, all tubes were kept at room temperature.

2.5.3. Agarose gel electrophoresis.

In the first SELEX cycle, PCR product was resolved on 4% agarose gel which was prepared by dissolving UltraPure™ agarose powder (Cat. No. 16500500; Invitrogen, Rockford, IL, USA) in TAE buffer (40 mM Trizma base; 20 mM glacial acetic acid, 1 mM EDTA, pH 8.3). The suspension was heated in a microwave in 10-15-second pulses to facilitate agarose powder dissolution. Once prepared, the agarose solution was kept liquid at +70°C.

To cast one ~ 4 mm thick gel, liquid agarose solution was poured into a clear 7 x 7 cm casting tray with 1.00 mm comb inserted. After 20 minutes, the polymerised gel in its tray was placed into a horizontal electrophoresis cell (Owl EasyCast B1 mini gel electrophoresis system, Thermo Scientific) and submerged in TAE buffer.

DNA samples were prepared by combining 10 µL of the PCR product from each reaction with 2 µL of TrackIt cyan/yellow loading dye (Cat. No. 10597012; Invitrogen, Vilnius, Lithuania). The wells were loaded with 10 µL of each sample and Ultra low range DNA ladder (Cat. No. 10597012; Invitrogen, Vilnius, Lithuania). The electrophoresis was performed at 80 volts for 60 minutes.

Next, the gel was stained for 10 minutes with GelStar nucleic acid gel stain (Lonza, Rockland, ME, USA) followed by a wash with deionised water for 20 minutes. The resolved bands were visualised with Fusion Fx imaging platform and software (Vilber Lourmat, France).

2.5.4. Aptamer amplification for the next round of selection.

Once the optimal number of cycles was determined, the remaining selected aptamers were amplified using the standard PCR program (Table 4) by preparing 50 µL reactions (Table 3) in Axygen® 8-strip PCR tubes.

2.6. Denaturing polyacrylamide gel electrophoresis.

To cast one 12.5% 8M urea polyacrylamide gel, a solution was prepared by combining 3,125 µL of 40% SureCast™ acrylamide (Cat. No. HC2040; Life Technologies, Carlsbad, CA, USA), 4.8 g of urea, 1 mL of 10 M TBE buffer (890 mM Trizma base, 20 mM EDTA, 890 mM boric acid, pH 8.0) and MilliQ water to a total volume of 9.96 mL and gently heating in a 40°C water bath for 5-10 minutes to dissolve urea. Once the solution was uniformly transparent, it was cooled to room temperature before adding 33 µL of 30% ammonium persulfate. 30% ammonium persulfate was prepared by dissolving 300 mg of SureCast™ ammonium persulfate (Cat. No. HC2005; Life Technologies, Carlsbad, CA, USA) in 1 mL of MilliQ water and stored as 40 µL

aliquots at -20°C. The polyacrylamide solution was mixed by inversion, and 4 µL of SureCast™ TEMED (Cat. No. HC2006; Life Technologies, Carlsbad, CA, USA) was added and gently mixed by inversion. The solution was immediately poured into a 1.5 mm thick casting cassette (Bio-Rad) and fitted with 1.5 mm 5-well comb (Bio-Rad) or a 1.0 mm thick casting cassette (Bio-Rad) and fitted with 1.0 mm 10-well comb (Bio-Rad). The gel was left to polymerise for 15 minutes. Once set, the casting cassette was removed from its holder and inserted into an electrophoresis Mini-Protean® tetra cell (Bio-Rad) opposite another gel or a buffer dam. The internal chamber was filled with 1 M TBE buffer (89 mM Trizma base, 2 mM EDTA, 89 mM boric acid, pH 8.0), while the cell was filled with the same buffer to the "2 Gels" mark (~500 mL total buffer volume). If three or four gels were run simultaneously, the tank was filled to the "4 Gels" mark (~1 L total buffer volume). The well-comb was removed, and the wells were flushed with the surrounding buffer using 1000 µL pipette to remove urea precipitate. The gel was pre-warmed by running the electrophoresis at 15 watts for 30 minutes.

Meanwhile, equal volumes of PCR product (dsDNA) and formamide loading buffer (63% formamide; 0.5 mM EDTA, 0.0003% xylene cyanole, 0.00065 % bromophenol blue, 0.0003% orange G) were combined in 1.5 mL Eppendorf tubes and heated at 95°C for 10 minutes to denature DNA. An unamplified positive control was prepared by combining 0.6 µM initial aptamer library with an equal volume of formamide loading buffer and heating at 95°C for 10 minutes. The control was included in one gel only per each SELEX cycle.

Once the gel was pre-warmed, the wells were flushed twice with the surrounding buffer using 1000 µL pipette to remove any further urea precipitate that might have formed. The five-well gels were loaded with 158 µL of sample per well while the ten-well gels were loaded with 28 µL of sample per well. All unoccupied wells were filled with loading buffer diluted with an equal volume of MilliQ water. The electrophoresis was run at constant 15 watts for 25-35 minutes until the dye travelled to the bottom edge of the gel. Once complete, the gel was removed from the

cassette and stained for 10 minutes with GelStar nucleic acid gel stain (Lonza, Rockland, ME, USA), followed by a 10-minute wash with deionised water. To avoid the damaging effects of the ultraviolet light on DNA and introducing mutations into the oligonucleotide library, the gel was viewed with a Dark Reader blue LED transilluminator (Clare Chemical Research, Dolores, CO, USA).

2.7. Electroelution from polyacrylamide gel.

Pur-A-Lyzer™ midi dialysis tubes (3.5K molecular weight cut off; Cat. No. PURD35050; Sigma-Aldrich) were filled with 800 µL UltraPure™ DNase/RNase-free distilled water (Cat. No. 10977015; Invitrogen, Rockford, IL, USA) to hydrate the membranes. After five minutes, one slice of gel containing the selected aptamers was added to each tube. The lids were carefully closed to avoid introducing air bubbles. The tubes were inserted into a holding tray and oriented so that the membranes were perpendicular to the electric current. The tray was placed in a horizontal electrophoresis tank (Cleaver Scientific, UK) and submerged with 0.5 M TBE buffer (44.5 mM Trizma base, 1 mM EDTA, 44.5 mM boric acid, pH 8.0). The electrical current was applied at a constant 100 V for 45-50 minutes. The process of elution was monitored by viewing the gel slices inside the tubes with blue LED transilluminator (Clare Chemical Research, Dolores, CO, USA). Once no more dye could be seen inside the gel, the tubes were placed back into the electrophoresis tank, and the polarity of the electric current was reversed for two minutes at 100 V to release the DNA from the membranes. Upon completion, the tubes were carefully opened, and the eluate was pipetted five times before being transferred into a 1.5 mL Eppendorf tube. The eluate was concentrated in a Genevac miVac (Scitek) rotational vacuum concentrator at 56°C for 35 minutes to achieve the final volume of 50 µL.

The dialysis tubes were used multiple times within the same experiment. They were stored at room temperature filled with 800 µL UltraPure™ water and submerged into TBE buffer.

2.8. Ethanol precipitation of oligonucleotides.

Two methods of ethanol precipitation of the eluted oligonucleotides were trialled. In the first instance, the sample was combined with 1/10th volume of 1 M ammonium acetate and two volumes of absolute ethanol. The eluant solution was incubated at -20°C for 48 hours. After incubation, the mix was centrifuged (Allegra 64R, Beckman Coulter) at 21,000 RCF at 4°C for 40 minutes to pellet the DNA. The supernatant was removed and discarded while 500 µL of cold 70% ethanol was added to the DNA/salt pellet, mixed with a pipette and centrifuged at 21,000 RCF at 4°C for 10 minutes to pellet the clean DNA. The supernatant was once again removed and discarded, and the pellet was left to dry out for 10-15 minutes. The DNA was then resuspended in 50 µL of UltraPure™ water.

In the second instance, the sample was combined with 1/10th volume of 3 M sodium acetate and incubated for 15 minutes. Next, two volumes of absolute ethanol were added to the eluant and incubated at -20°C for 2 hours. After incubation, the centrifugation, washing, drying and resuspension steps were performed as before.

2.9. Zymo oligo clean and concentrator kit.

Purification of the eluted aptamers was performed with Zymo® oligo clean and concentrator kit (Cat. No. D4060; Zymo Research, USA) following the manufacturer's instructions. For this, 50 µL of sample was combined with 100 µL of binding buffer in a 1.5 mL Eppendorf tube and mixed with a pipette. 400 µL of absolute ethanol at room temperature was added and mixed with a pipette. The solution was transferred into a spin column inserted into a collection tube and centrifuged (Microfuge 16, Beckman Coulter) at 10,000 RCF for 30 seconds. The supernatant was discarded, and 750 µL of the washing buffer was added to the spin column. The column was centrifuged at 10,000 RCF for 30 seconds, followed by another centrifugation at 16,000 RCF for 1 minute. The flow-through in the collection tube was again discarded. The spin column was transferred into a 1.5 mL Eppendorf tube, and 15 µL of UltraPure™ water was added directly to

the filter. The spin column was once again centrifuged at 10,000 RCF for 30 seconds. The collected supernatant containing clean aptamers in water was analysed by NanoDrop ND-1000 spectrophotometer to determine the final aptamer concentration in the solution.

2.10. NanoDrop DNA quantification.

Oligonucleotide quantity and purity was determined by analysing 2 μL of a sample with NanoDrop ND-1000 spectrophotometer. Prior to loading on the spectrophotometer, the samples were warmed up to 37°C in the water bath to ensure consistency as the temperature can greatly affect absorbance values. The absorbance was analysed by NanoDrop 1000 software version 3.7.1.

CHAPTER 3. Results and discussion.

3.1. Patients' sera screening with anti-cN1A ELISA.

A diagnostic ELISA for the detection of circulating anti-cN1A antibodies was developed in 2016.[4] The assay is an indirect type of ELISA where serum circulating antibodies are captured by the immobilised cN1A protein (Figure 9). Bound antibodies are then detected indirectly by

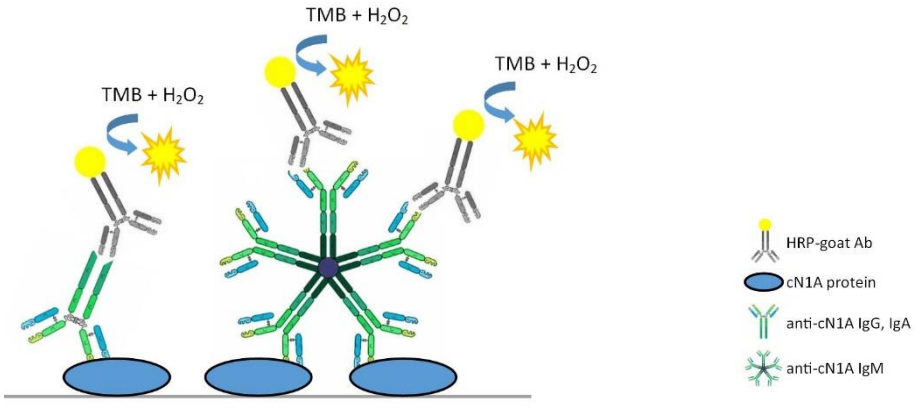

Figure 9. Indirect anti-cN1A ELISA. Serum is challenged with immobilised cN1A protein. Bound anti-cN1A antibodies are detected by HRP-conjugated goat anti-human antibodies via colourimetric reaction of HRP with H_2O_2 in presence of TMB.

horseradish peroxidase (HRP)-labelled secondary antibodies. HRP is an enzyme that catalyses the oxidation of TMB by hydrogen peroxide resulting in the production of blue colour which can be detected at 650 nm. Detection of the primary reaction colour, however, can introduce undesired well-to-well variability into the assay as it continues to develop over time with no true endpoint. Therefore, sulphuric acid stop solution is used to terminate the reaction after 10 minutes consistently for each well. Upon the acid addition, the colour changes to yellow with the absorption maximum at 450 nm.

The absorbance measurement represents the amount of light intensity lost when it passes through the sample well (Figure 10). If the light intensity (I) of the serum-containing well is less than the light intensity of the well containing all the other ELISA components but no serum (I_0), then the sample has absorbed some of the light (Equation 3).

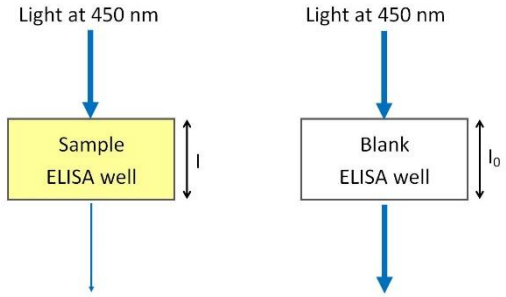

Equation 3. ELISA sample absorbance.

$A = I - I_0$, where

A – sample absorbance

I – the light intensity of the sample well

I_0 – the light intensity of the blank well

Figure 10. Light at 450 nm absorbed by the sample and blank ELISA wells. I, I_0 = change in light intensity.

In the semi-quantitative ELISA performed, the sample absorbance was calculated relative to the absorbance value obtained from the healthy sera pool.

Initially, the ELISA was developed to detect IgG antibodies only by using secondary antibodies that were raised to specifically recognise human IgG. However, it has been shown that circulating anti-cN1A antibodies comprise of IgG, IgA and IgM isotypes.[42] Hence, in the present experiment, the variety of the secondary antibodies was expanded to include IgG, IgA and IgM recognition in addition to the so-called "pan" detection antibodies that were not isotype specific.

A cohort of forty-eight patients with clinically diagnosed IBM was analysed by the anti-cN1A ELISA. Reactivity against cN1A was detected in eighteen patients (38%) (Figure 11). This finding is comparable with the previously reported data where on average 55% (35.5%-80%) of IBM patients were found seropositive with the cN1A ELISA (Table 1).

Regarding specific isotypes, six patients were seropositive for IgG only (33% of seropositive

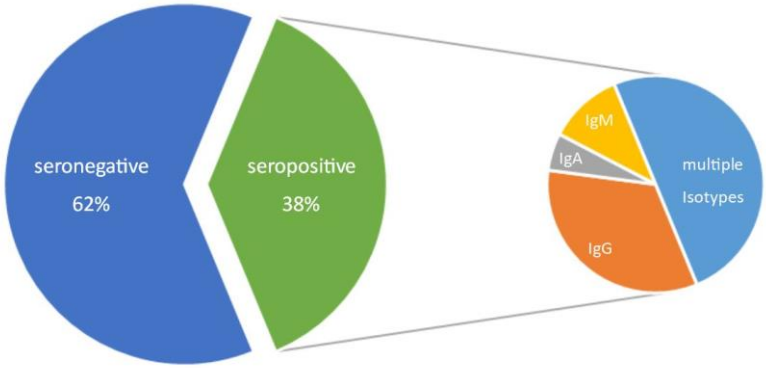

Figure 11. Anti-cN1A status of IBM patients as determined by the ELISA (n = 48). Seropositive absorbance ratio cut-off values: IgG/M/A >= 2.5; IgG >= 4.2; IgM >=2.3; IgA >= 5.4

patients), one for IgA only (6%) and two for IgM only (11%). The remaining 50% of patients had multiple autoantibody isotypes present at above the normal ranges.

The patient selected for donating blood for anti-cN1A purification was assayed positive for IgG (absorbance ratio = 11.0), IgA (absorbance ratio = 39.1) and IgM isotypes (absorbance ratio = 2.5).

3.2. Anti-cN1A purification from IBM serum.

Serum anti-cN1A purification was achieved by capture with cN1A-coated magnetic beads. The process of cN1A protein conjugation to magnetic beads utilises a cobalt-based immobilised metal-affinity chromatography (IMAC) chemistry, where cobalt ions immobilised on magnetic polymer beads bind recombinant proteins containing a short polyhistidine tag.[72] Out of all the amino acids, histidine forms the strongest interaction with cobalt ions which is stable at neutral pH but can be disrupted at low pH of ~6.0. By using near-neutral pH buffers for the antibody purification, I was able to keep cN1A conjugated to the beads throughout the entire purification process. Cycles of serum depletion were repeated until the absorbance values obtained by the ELISA for the depleted serum were within 10% of the blank well containing no serum. Purification under native conditions and elution of the captured antibodies with a gentle elution buffer yielded biologically active purified anti-cN1A. Their affinity for the target protein was confirmed by the ELISA, which produced concentration-dependent absorbance values with a maximum of 0.73 (Figure 12).

Purified anti-cN1A antibodies were resolved on SDS-PAGE alongside the commercial biotinylated goat IgG (Figure 13). Goat IgG at ~147 kDa including the biotin label (Figure 13, 6) was used as a positive control and a weight marker. While a single band was expected for the commercially purified IgG, two additional bands can be observed – one of ~55 kDa (Figure 13, 7) corresponding to the immunoglobulin heavy chain and one of ~25 kDa (Figure 13, 8)

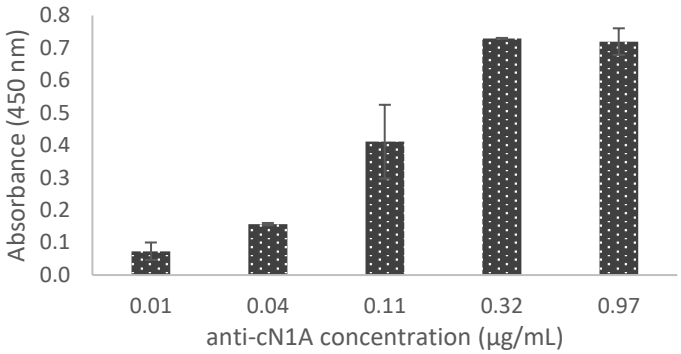

Figure 12. ELISA to determine purified anti-cN1A biological activity. Wells were coated with 20 µg/mL cN1A protein. Bound antibodies were detected with goat anti-human horseradish peroxidase (HRP)-conjugated antibodies against IgG/M/A and visualised via TMB substrate reaction at 450 nm. Mean of duplicate measurements are plotted. Error bars represent standard deviation.

corresponding to the light chains. These bands are evidence of some degree of degradation presumably due to the extended storage time of the sample.

The bands from non-reduced human immunoglobulins were not well defined due to a heterogenous mix of isotypes and clones of anti-cN1A (Figure 13, non-reduced). Nevertheless, I can identify a band at the top (Figure 13, 1) produced by a heavy protein, likely IgM, that did not migrate into the resolving gel during the electrophoresis. A faint band at ~162 kDa (Figure 13, 2) corresponds to a small amount of IgA. The widest band covers a range of ~150 to ~50 kDa (Figure 13, 3). This band may contain complete IgG of ~150 kDa as well as some

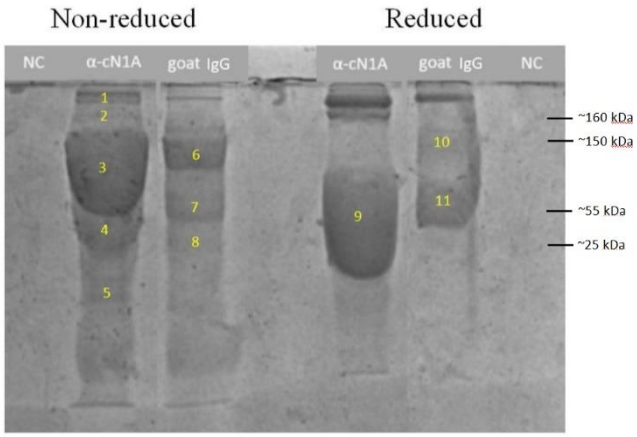

Figure 13. Resolution of purified polyclonal anti-cN1A and goat IgG on gradient SDS-PAGE. 6 µL of anti-cN1A and 3.5 µL of goat IgG were combined with equal volumes of non-reducing or reducing (0.35 mM DTT) loading buffers. Electrophoresis was performed at 90 volts for 1.45 hours. NC – loading buffer only.

immunoglobulin heavy chains ~55 to ~65 kDa. A band corresponding to immunoglobulin light chains of ~25 kDa (Figure 13, 4) can be found directly below it. The appearance of these bands provides evidence of some degree of anti-cN1A degradation that could have been resulted from any step of the purification process. The fraction of the degraded ant-cN1A is, however, small and should not have any significant consequences for the selection process. The nature of the two faint bands of less than 20 kDa (Figure 13, 5) could not be identified.

The presence of DTT in the reducing buffer combined with heating of the samples to 95°C caused denaturation of the proteins by cleaving the disulfide bridges. It is evident by the presence of the faint band of ~144 kDa (Figure 13, 10) that denaturation conditions were insufficient to completely reduce goat IgG. The other band (Figure 13, 11) corresponds to the IgG heavy chain of ~55 kDa. The light chains cannot be observed.

Reduced anti-cN1A sample produced one wide band stretching from ~55 to ~23 kDa (Figure 13, 9) presumably containing light and heavy chains, although they cannot be distinguished from each other.

To conclude, the resolution of anti-cN1A on SDS-PAGE has provided evidence of a small degree of degradation that the protein suffered during the purification process. The segregated heavy and light chains will not present an obstacle for the selection process since they will be readily eliminated by the first capture step of SELEX.

The final concentration of the purified anti-cN1A was determined by the colourimetric BCA protein assay. The assay relies on the conversion of Cu^{2+} to Cu^{1+} ions by a protein in an alkaline medium. The generated Cu^{1+} ions react with bicinchoninic acid (BCA) to produce a purple-coloured product with an absorbance maximum at 562 nm (Figure 14).[73]

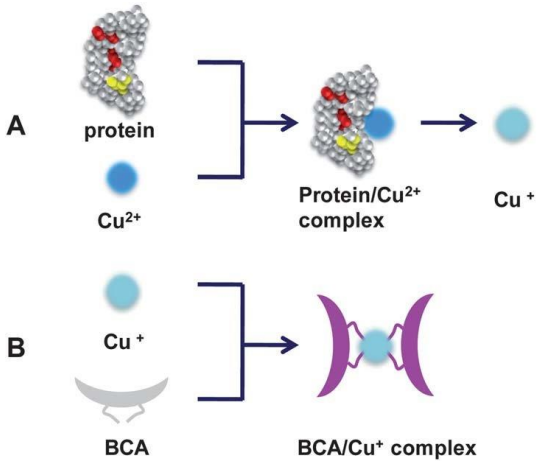

Figure 14. BCA reactions chain: A. chelation of Cu^{2+} with protein to produce Cu^{1+}; B. formation of purple colour by the BCA/ Cu^{1+} complex. Image source: Bing Zhao @ Researchgate.

In the current experiment, the quantification of purified anti-cN1A was achieved by a direct comparison to the set of BSA standards of known concentrations up to 2000 µg/mL that were assayed under the same conditions as the sample (Figure 15). The near-linear increase of

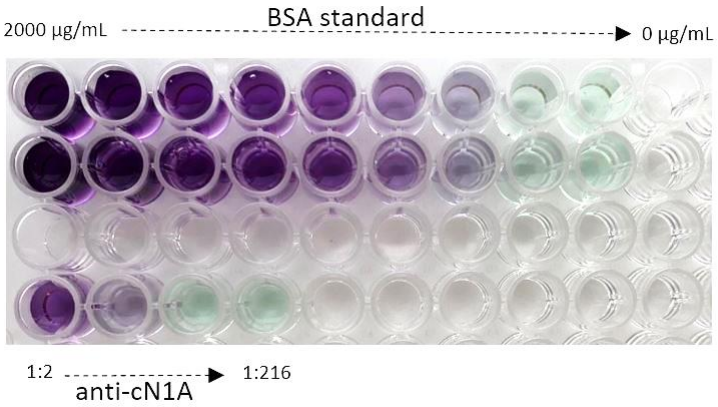

Figure 15. The bicinchoninic acid (BCA) assay for anti-cN1A antibodies quantitation. Colour response of the bovine serum albumin (BSA) standard titrated from 0 to 2000 µg/ and titrated anti-cN1A samples.

absorbance with the increased protein concentration enabled a construction of a standard colour response curve (Figure 16). Two sample absorbance measurements corresponding to 1:2 and 1:7 anti-cN1A dilutions were placed within the colour response curve and used in the equation. The concentration of the anti-cN1A antibodies was determined to be 970 ± 59 µg/mL. The total amount of purified anti-cN1A antibodies was 6.5 mg.

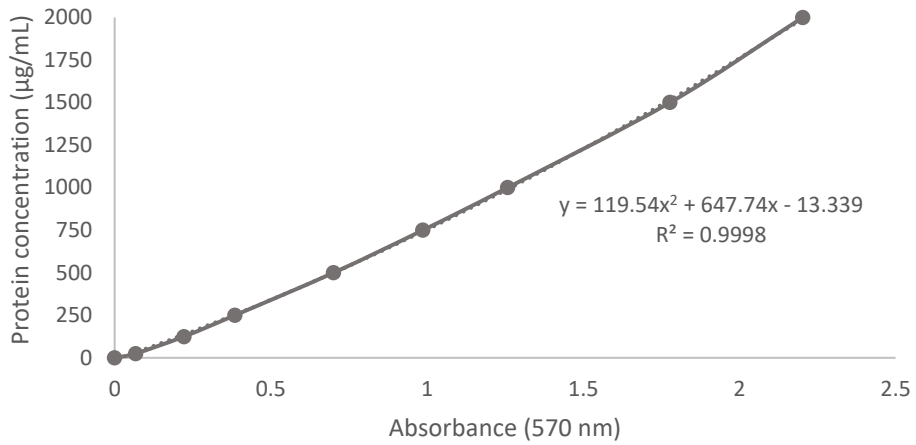

Figure 16. The colour response curve of the bovine serum albumin standard constructed from duplicate values. Mean absorbance for each sample was adjusted to the mean of blank (working reagent only). Absorbance values are presented on the x axis for the ease of further calculations. The curve is fitted with a polynomial trendline. The equation where y represents protein concentration and x represents absorbance is used to calculate the anti-cN1A concentrations: $y = 119.54x^2 + 647.74x - 13.339$

3.3. *In vitro* SELEX.

The primary aim of this project was the selection of aptamers that can neutralise anti-cN1A binding to their target protein. The process used for the *in vitro* development of such aptamers followed a modified procedure based on the standard SELEX framework described in Section 1.4.1. Two SELEX cycles were performed during this study, each consisting of the consecutive steps of the aptamer library incubation with anti-cN1A antibodies; isolation of the neutralising aptamers; aptamer amplification; DNA strand separation; and aptamer purification.

Each step will be reviewed in detail in this section.

3.3.1. Capture SELEX for the neutralising aptamers isolation.

One of the prerequisites to a successful SELEX is the separation of bound and free aptamers. Traditionally, such separation is enabled by immobilisation of a selection target to a solid phase, such as microfluidic slips, magnetic chips, agarose-based resin or magnetic beads.[62] Our approach was to isolate specific antibody/DNA complexes where the aptamer was interacting with the antibody's binding site. To achieve this, we chose to immobilise the antibodies' protein target - cN1A - to a 96-well ELISA plate. Only free antibodies or those targeted by aptamers outside of the binding site can interact with cN1A and remain captured in the well, while the supernatant containing specifically-bound and free aptamers is removed and retained. To ensure that most non-neutralising aptamers are removed from further selection, it was necessary to determine anti-cN1A concentration at which most of the circulating antibodies are captured by the immobilised cN1A.

The optimum anti-cN1A concentration was determined by the ELISA with serially titrated anti-cN1A antibodies. Each dilution was successively incubated twice with the target protein (Figure 17). Mean absorbance values obtained from each incubation were plotted against the

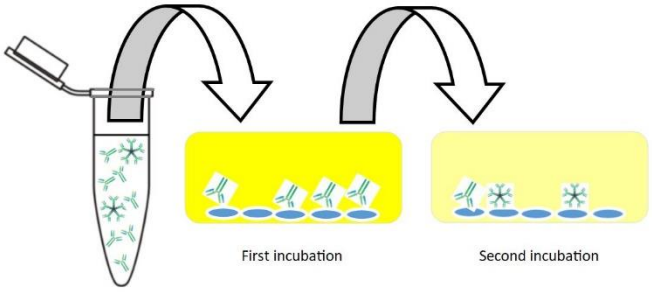

Figure 17. Schematic representation of the ELISA to determine optimum anti-cN1A concentration for capture with 20 µg/mL cN1A. Each dilution of anti-cN1A was consecutively incubated in a cN1A-coated well for two hours.

corresponding antibody concentrations (Figure 18). The data presented shows that cN1A binding sites saturation is achieved at anti-cN1A concentration of 0.32 µg/mL as evidenced by the

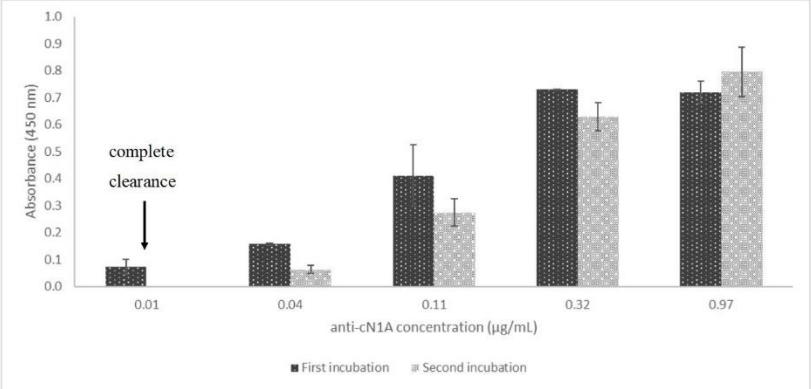

Figure 18. ELISA to determine anti-cN1A concentration at which complete clearance can be achieved. Wells were coated with 20 µg/mL cN1A protein. Anti-cN1A (970 µg/ml) were serially titrated as 1:1000, 1:3000, 1:9000, 1:27,000, 1:81,000 and consecutively incubated inside coated wells twice for 2 hours at room temperature. Bound antibodies were detected with goat anti-human horseradish peroxidase (HRP)-conjugated antibodies against IgG/M/A and visualised via TMB substrate reaction at 450 nm. Mean of duplicate measurements are plotted. Error bars represent standard deviation.

plateauing maximum absorbance value of ~0.7. It is unclear, however, why there is an incomplete capture of the antibodies at the concentrations much lower than that of the cN1A binding saturation. Even at 0.04 µg/mL, there is a transfer of uncaptured antibodies into the second incubation well (Figure 18). Could it be due to the polyclonal nature of the antibodies so that the increased concentration results in competition between the anti-cN1A molecules and favours binding of the clones with the highest affinity and avidity for the target? Current data is insufficient to support this hypothesis; however, exploring the molecular mechanisms underlying this result could offer further insights into the nature of the anti-cN1A interaction with their target.

According to the data presented here, complete clearance of the antibodies was achieved at 0.01 µg/mL corresponding to 1:81,000 dilution (Figure 18). Such low concentration, however, was impractical for SELEX as each capture step would require a large number of coated ELISA plates to complete the selection. Therefore, concentration of 0.1 µg/mL corresponding to 1:10,000 dilution was arbitrarily selected for the early rounds of SELEX capture. Consideration was given to the fact that some non-specific aptamers might be carried over to the next selection

cycle; however, in theory, they would be subsequently removed during the repeated capture SELEX steps.

The separation of antibody/aptamer complexes and free aptamers was another critical step in the SELEX process. In the first instance, we planned to resolve the supernatant on a native polyacrylamide gel and identify bound antibodies by the shift in the electrophoretic mobility.[74] Given that we were targeting polyclonal antibodies of many isotypes, and their mobility on the gel was dependent not only on their molecular weight but also on the electrical charge and tertiary structure of the individual immunoglobulin molecules, it would have been extremely challenging to obtain a sufficiently high resolution to observe the shift. Additionally, it has been shown that upon aptamer binding, individual proteins may undergo conformational changes that result in further reduction in gel resolution.[75] Thus, we chose to capture anti-cN1A/aptamer complexes with streptavidin magnetic beads interacting with biotinylated anti-human antibodies. The interaction of biotin with a bacterial protein streptavidin is one of the strongest non-covalent reactions in nature. It has numerous application in protein-ligand experiments due to its high specificity, fast reaction rate and stability under a wide range of conditions.[76] What's more, a comprehensive array of biotinylated proteins is commercially available for molecular applications.

In this stage of SELEX, biotinylated goat anti-human antibodies raised against IgG, IgA and IgM isotypes, formed conjugates with aptamer-bound anti-cN1A antibodies and were subsequently captured by Dynabeads® covered in a single streptavidin layer. During a short incubation, the streptavidin-biotin interaction occurred allowing the separation of the selected antibody-bound aptamers from unbound oligonucleotides.

3.3.2. Selected aptamers amplification.

While the clearance of magnetic beads was not strictly required for the amplification, we chose to elute the aptamers off the beads by heat denaturation and remove the beads from the

suspension using a magnet. The precleared suspension containing the selected aptamers was then PCR amplified.

The PCR method developed by Kary Mullis in 1983 is based on the ability of a DNA polymerase to synthesise a DNA strand complementary to the provided DNA template.[77] Most polymerases are strictly limited to adding free bases to an existent 3′ hydroxyl group. Therefore, annealing of a synthetic primer comprising a specific oligonucleotide sequence is necessary to create a starting point for the extension by the polymerase.

In the current SELEX procedure, the initial DNA library was synthesised to include specific primer-binding sites at each end of the random sequence, and the primers of complementary sequences to those binding sites were produced (Figure 19). The forward primer additionally

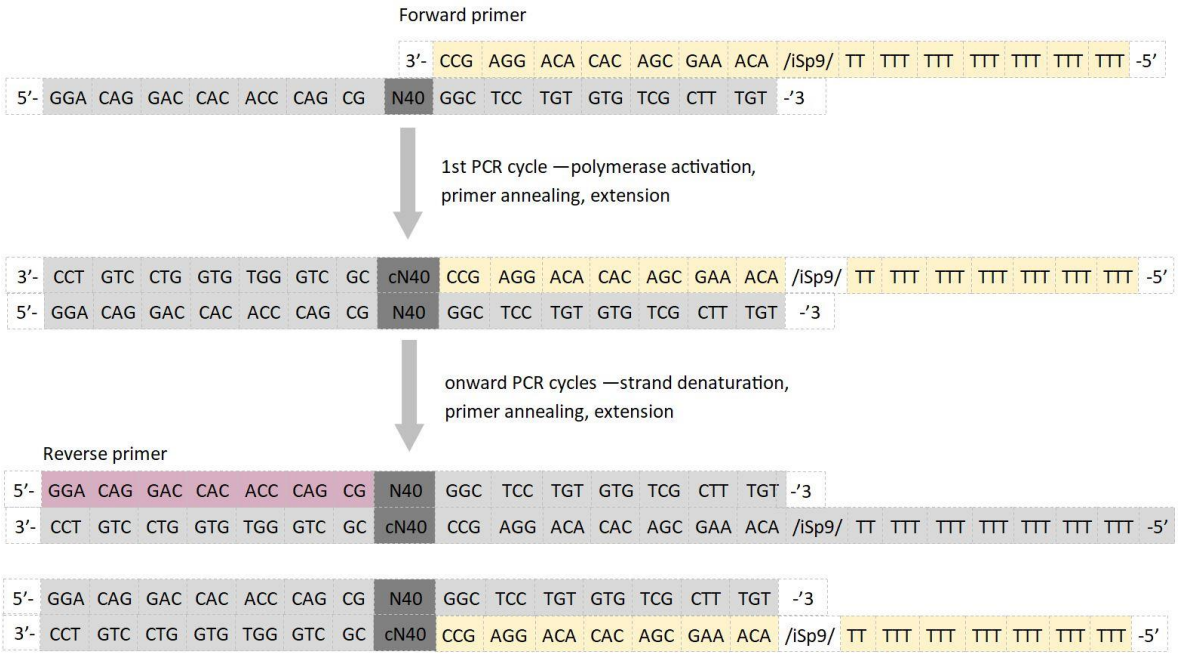

Figure 19. PCR amplification of the selected aptamers using asymmetric primers. N40 is the random sequence of 40 nucleotides; cN40 is the complementary random sequence of 40 nucleotides; iSp9 is a linker.

features a poly-T tail conjugated to the main sequence by an iSp9 linker. During the extension of the sense strand from the reverse primer, the iSp9 linker serves as a terminator for the polymerase. In this way, the generated double-stranded PCR product contains asymmetric strands - the sense strand of 81 nucleotides of the identical sequence to the initial library, and the irrelevant anti-sense strand of 101 nucleotides of the complementary sequence. The difference

in primer lengths is necessary for the separation of the sense- and the anti-sense DNA strands discussed in section 2.6.

The choice of a polymerase was an important consideration for the SELEX outcome. In the past, the preference was given to error-prone polymerases that had high mutation rates. This choice was targeted at increasing the aptamer pool sequence diversity by introducing random mutations.[62] However, it was also noted that error-prone polymerases added uncertainty and less control over the selection process. Given that our initial aptamer pool already contained over 10^{16} sequences, the complications of introducing mutations outweighed the benefits of additional diversity; hence, a high-fidelity polymerase was chosen for the amplification. Phusion DNA polymerase mix with HF buffer used in this project has a reported mutation rate of 1.81×10^{-6}, which was the lowest among the six high-fidelity polymerases investigated by Hestand *et al.*[78]

3.3.3. The importance of analytical PCR.

An issue that consistently arises in SELEX studies is the formation of unwanted by-product (sometimes termed "parasitic DNA") during PCR amplification. This phenomenon was investigated by Tolle *et al.*[79] In their work, the authors observed a formation of two types of by-products they termed the ladder-type and non-ladder type that were both longer than the expected DNA product. In the first round of SELEX, I similarly observed these two kinds of by-products (Figure 20). Tolle *et al.* suggested possible mechanisms that could explain such by-product

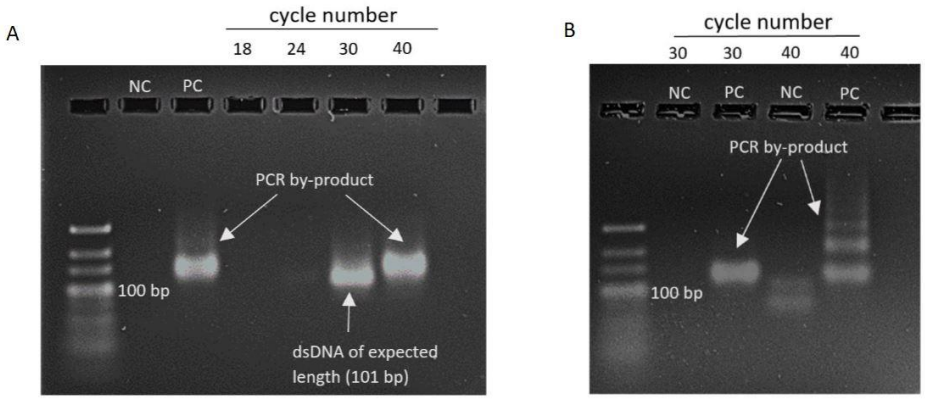

Figure 20. Resolution of PCR product on 4% agarose gel under 100 V electrophoresis showing a non-ladder (A and B) and a ladder-type (B) by-products. PC – positive control of the initial oligonucleotide library at 10 µM; NC – negative control containing no DNA template.

formation.[79] In their hypothesis, both events are initiated by one of the primers binding to a region within the random sequence and being elongated by the polymerase (Figure 21). One of the

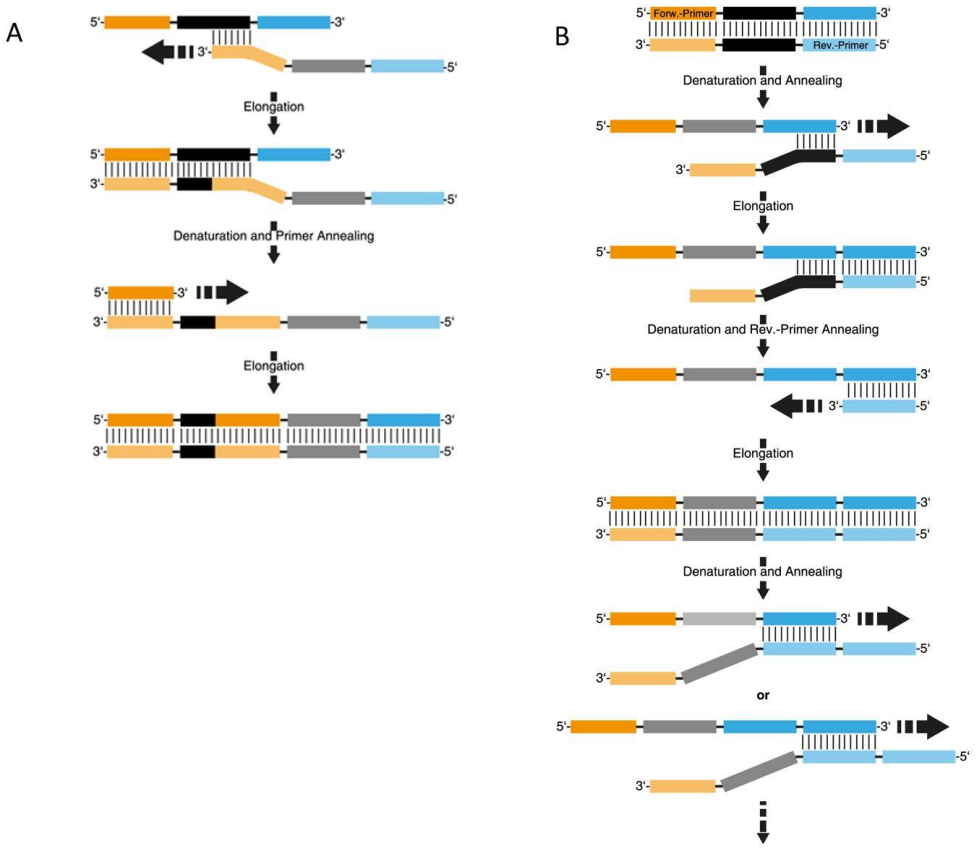

Figure 21. Mechanisms of the non-ladder (A) and ladder (B) type PCR by-product formation proposed by Tolle et al.

events can lead to a duplication of a primer-binding site resulting in an ever-increasing by-product length, seen as ladder-type bands (Figure 20, B). However, if the primer binds within the random region but does not create an entirely new binding site, the resulting by-product will be longer but will not be infinitely extended. Such by-product will subsequently produce non-ladder type bands (Figure 20, A).

Tolle *et al.* observed the formation of the parasitic DNA throughout the entire SELEX. It was demonstrated by these authors and others that the appearance of the by-product formed a PCR bias where it was preferentially amplified by the polymerase and resulted in dominating the selection pool compromising the success of SELEX.[79, 80] I was pleased not to encounter any parasitic DNA in the second round of selection. Possible reasons for this observation could be

the elimination of all the sequences that were structurally able to form by-product in the first selection round, as well as a lower DNA concentration of the template which led to the consumption of the PCR reaction reagents earlier in the amplification cycles (Figure 22, A).

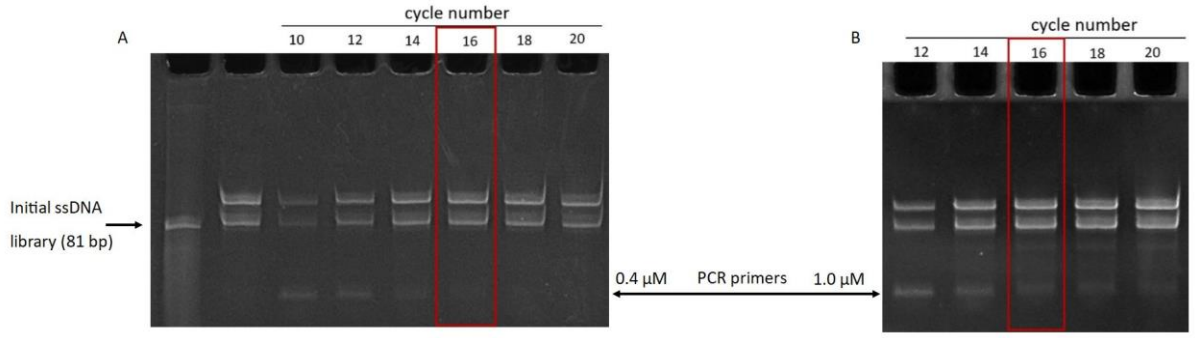

Figure 22. Resolution of the analytical PCR product on denaturing 12.5% 8M urea polyacrylamide gel. PCR was performed with 0.4 µM primers per 50 µL reaction (A) or 1.0 µM primers per 50 µL reaction (B). In both cases 16 cycles of amplification produced the optimum amount of ssDNA of 81 bp.

To investigate whether the concentration of primers in the reaction mix was the limiting factor for the maximum amount of PCR product that could be achieved, I increased the primers fraction from 0.4 µM to 1 µM per 50 µL reaction. Upon resolution of the PCR product on a polyacrylamide gel, I still observed the plateau in the amount of the amplified product after the 16th cycle (Figure 22, B). Therefore, I concluded that the concentration of dNTPs in the reaction mix was the limiting factor in the final amount of the amplified DNA product, and 0.4 µM was carried over as the optimum primer concentration for amplification of the selected library.

Of note, I chose to visualise the PCR product on polyacrylamide gel in the second SELEX round because of its higher resolution than agarose gel. Since the concentration of DNA obtained in the second round was much lower than in the first, polyacrylamide gel was more suitable to observe even a small amount of by-product if there was any present.

To conclude, optimisation of the amplification cycles in the first round of SELEX was aimed at maximising the amount of DNA of the expected size while minimising the amount of PCR by-product formed. In the second round, however, the optimisation was primarily directed at maximising the amount of DNA obtained while consuming the least PCR reagents.

3.3.4. PCR amplification bias.

Upon resolution of the amplified DNA on dPAGE in every round of SELEX, it was noted that the sense strand was preferentially amplified resulting in 21-29% more PCR product (Figure 23).

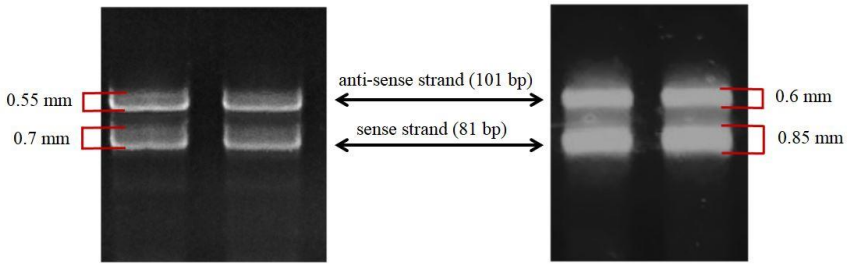

Figure 23. Examples of PCR amplification bias towards the selected aptamers. PCR products obtained in the 1st and 2nd rounds of SELEX were resolved on 12.5% 8M urea polyacrylamide gel.

While some SELEX protocols integrate a feature of asymmetric amplification where one primer is used in higher concentration than the other, our PCR was performed with equal amount of the forward and the reverse primers in each reaction. The efficiency of the PCR amplification was likely influenced by the effectiveness of the primer annealing that can be dictated by many factors, including primer length, molecular weight, melting temperature and GC content. Characteristics of the primer pair used for the amplification are presented in Table 5. The higher melting temperature of the reverse primer at 66.6°C versus 64.6°C suggests a more stable binding to the DNA template resulting in higher amplification efficiency.

Table 5. Physical characteristics of the PCR primers used for amplification with Phusion DNA polymerase (calculated using Thermo Scientific Tm calculator).

	Forward primer	**Reverse primer**
Sequence	5′-ACAAAGCGACACACAGGAGCC-3′	5′-GGACAGGACCACACCCAGCG-3′
Length (bp)	21	20
Molecular weight (g/mol)	6427.2	6106.0
Tm (°C)	64.6	66.6
GC (%)	57.14	70.00

3.3.5. Amplified DNA strand separation.

It was essential to separate the sense- and the anti-sense strands of the double-stranded PCR product since upon denaturation their complementary sequences would tend to reanneal into double-stranded molecules at ambient temperatures. In theory, tertiary structures of the double-stranded DNA would differ from the initially selected aptamers and would likely have a diminished affinity for the target.

The separation of the DNA strands is a common requirement for SELEX, and various methodologies have been developed to achieve this.[62] One of the most widely applied separation methods involves the incorporation of biotin into the anti-sense DNA strand through the forward primer biotinylation, and subsequent removal of this strand from the pool with streptavidin-conjugated magnetic beads. While this strategy is time-efficient and straightforward, it has been associated with an increased generation of a PCR by-product (previously discussed).[79] Therefore, in the current experiment, the strand separation was achieved by denaturing polyacrylamide gel electrophoresis (dPAGE). Polyacrylamide gel high resolution enabled the separation of the sense and the anti-sense DNA strands due to their 20-nucleotide length difference (Figure 19).

As an additional advantage, resolution of the PCR product on dPAGE permitted preclearance of the DNA from undesirable sequences and molecules, such as PCR by-products, unincorporated primers and PAGE loading dyes (Figure 24).

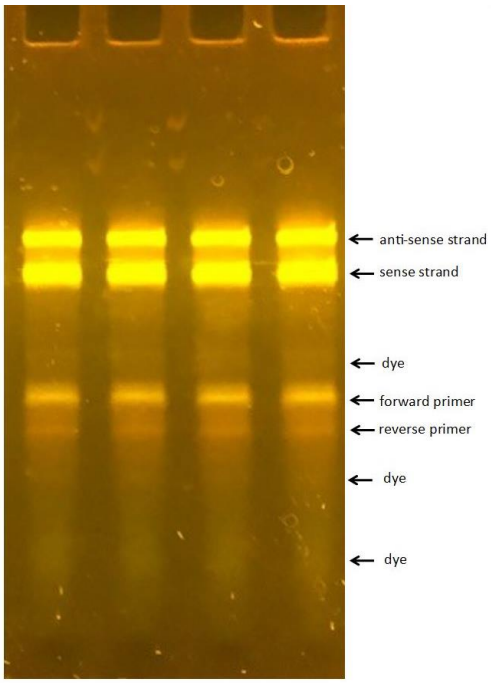

Figure 24. Resolution of the PCR product on denaturing 12.5% 8M urea polyacrylamide gel visualised under blue LED light. This method allows for the strand separation and preclearance of the amplified aptamers from undesired impurities such as unincorporated primers and loading dyes.

3.3.6. Selected aptamers purification from polyacrylamide gel.

Upon resolution on a polyacrylamide gel, the bands corresponding to the sense DNA strand were identified and excised from the gel requiring an elution step to free the DNA from the gel (Figure 25).

Traditionally, elution was performed by a "crush and soak" method developed in the 1970s, where agarose or polyacrylamide gel slices containing the sample were pulverised into a paste, and the DNA was diffused into an elution buffer over 18 to 36 hours.[81] Although not attempted

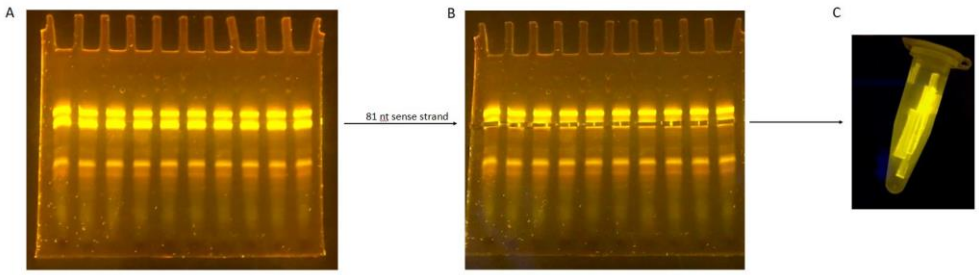

Figure 25. Stages of aptamer purification. A. PCR-amplified DNA was resolved on a 12.5% 8M urea denaturing polyacrylamide gel. B. 81-nucleotide sense strand was identified and excised from the gel. C. Aptamer-containing slices of gel were collected into a 1.5 mL Eppendorf tube.

during this experiment, the "crush and soak" method has been reported to recover as little as 30% to 50% of the sample DNA.[82] Additionally, crushing the gel may release various gel matrix material, such as water-soluble polyacrylamide molecules into the eluted sample and could interfere with the SELEX process.[83] Considering the small size of the oligonucleotides in our library, a simple passive diffusion from intact gel slices could be a viable alternative to the "crush and soak". Diffusion was attempted into either water or 1 M ammonium acetate. The elution process was monitored by examining the gel slices under the blue LED illuminator. After twenty-six hours, no oligonucleotides remained within the gel in the ammonium acetate elution tube, while it took thirty-six hours for the oligonucleotides to elute into water. Both samples were then ethanol precipitated using 1 M ammonium acetate salt. The precipitation resulted in a massive loss of aptamers – the concentration of DNA in the clean sample was below the NanoDrop detection limit (data not presented). A protocol from Harvard University suggested that oligonucleotides of less than 220 bases are refractive to precipitation in the presence of ammonium ions.[84] Subsequently, further precipitation experiments were carried out using sodium acetate.

Electroelution of aptamers from a polyacrylamide gel was also investigated in an attempt to decrease the elution time. The initial electroelution experiment was performed for 20 minutes at 120 volts in 1 M TBE buffer. As shown in Figure 26, A, these conditions were insufficient to withdraw the DNA out of the gel. Increasing the voltage to 200 for 10 minutes resulted in more,

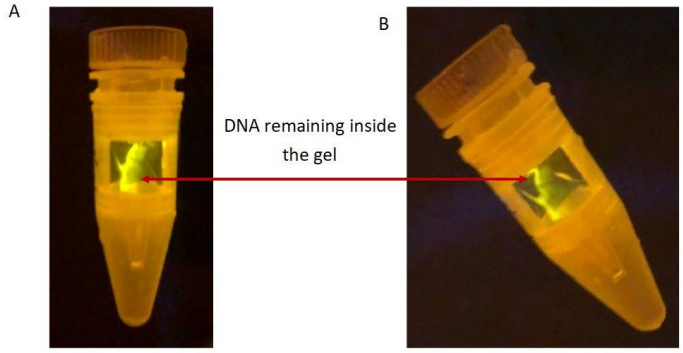

Figure 26. DNA remaining within the polyacrylamide gel slice after electroelution as seen under the blue LED light. A. Elution was performed at 120 volts for 20 minutes. B. Further elution was performed at 200 volts for 10 minutes.

but not all DNA exiting the gel (Figure 26, B). Complete DNA elution was achieved by increasing both the voltage to 200 volts and the elution time to 30 minutes. 4,200 ng of DNA was recovered via this method and ethanol precipitated with 3 M sodium acetate. Following the precipitation, only 635 ng of DNA was recovered (15% of the eluted fraction). I hypothesised that the increased salt concentration in the eluted samples due to warming of the elution buffer as a consequence of the increased voltage could have caused inefficient ethanol precipitation. Suboptimum precipitation conditions could have also been the cause. Optimisation of the ethanol precipitation protocol was not pursued further due to the limited amount of aptamers available for the experiments. Therefore, electroelution conditions were changed targeted at the reduction of salt contaminants. Complete elution of the DNA from the gel slices was achieved at 100 volts by extending the elution time to 45-50 minutes depending on the thickness of the gel slices and reducing the TBE buffer concentration to 0.5 M. Under these conditions, each 55 μL of the PCR product separated on the polyacrylamide gel yielded 3,800 – 4,200 ng of ssDNA.

Clean-up of the electroeluted aptamers was then attempted with Zymo oligo clean and concentrator kit. Since the kit has not been used by our laboratory before, it was essential to determine its ability to recover the oligonucleotides in our library and to optimise the purification conditions. For this, I performed a purification of the initial aptamer library while determining the DNA concentration before and after the process with NanoDrop spectrophotometer. In the initial experiment, the centrifugation was performed at 7,800 RCF, yielding a recovery rate of 70% (Figure 27). In the second experiment, the centrifugation speed was increased to 10,000 RCF, yielding a recovery rate of 92% (Figure 27). The optimised conditions were applied to two electroeluted aptamer samples, of which 81 and 93% were recovered (Figure 27).

Purification of aptamers marks the end of the selection cycle.

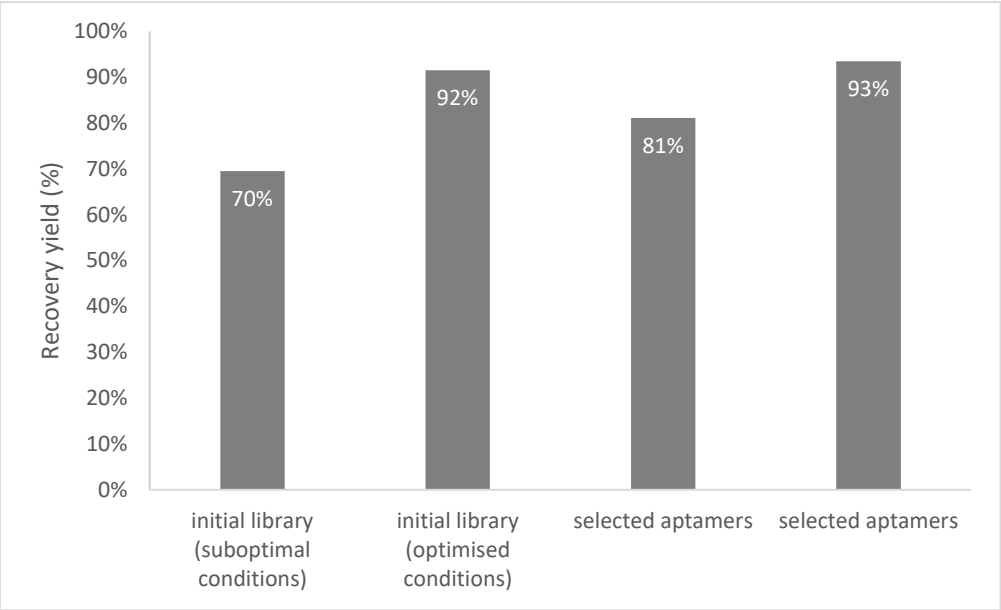

Figure 27. Aptamer recovery yield after purification with Zymo oligo clean and concentrator kit. 50 µL of either library or sample were combined with 200 µL of binding buffer and 400 µL of absolute ethanol. The samples were filtered by centrifuging at 7,800 x g (suboptimal) or 10,000 x g (optimal) for 30 sec. The samples were washed with 750 µL of washing buffer and centrifuged at 7,800 x g (suboptimal) or 10,000 x g (optimal) for 30 sec. To dry out, the samples were centrifuged for further 16,100 x g. Samples were collected into 15 µL of UltraPure water by centrifuging at 7,800 x g (suboptimal) or 10,000 x g (optimal) for 30 sec.

3.4. Determination of DNA quantity and quality with NanoDrop spectrophotometer.

All nucleic acids strongly absorb ultraviolet (UV) light at 260 nm. By determining the absorbance at 260 nm (A_{260}), DNA concentration in a sample can be calculated from the Beer-Lambert law (Equation 4).

Equation 4. The Beer-Lambert Law of light absorbance.

$A_{260} = \varepsilon_{260} cl$

where A_{260} – absorbance at 260 nm,

ε_{260} - extinction coefficient of the oligonucleotide at 260 nm in L mol^{-1} cm^{-1},

c - concentration in mol L^{-1},

l - pathlength in cm

As per the equation, the precise calculation of the DNA concentration depends on the knowledge of the exact extinction coefficient value, which is different for each of the four nucleotide bases. However, if the DNA sequence is unknown as it was in this study, NanoDrop calculates a sample DNA concentration by applying a constant for ssDNA based on the average extinction

Equation 5. NanoDrop calculation of the single-stranded DNA concentration.

$c = A_{260}*33$

where c - concentration in mol L^{-1}

A_{260} – absorbance at 260 nm

33 – ssDNA constant

coefficient for all four bases (Equation 5). The constant, therefore, assumes an even distribution of A, T, G and C, which is typically not the case with oligonucleotide sequences. Consequently, the concentration values obtained by NanoDrop for each sample are only indicative of the actual DNA concentration (Figure 28).

Additionally, NanoDrop provides two measures to assess DNA purity. The absorbance at 280 nm indicates the presence of proteins and other substances that absorb at this wavelength. In this study, the ratio of 260/280 of ~1.8 was considered high-purity DNA (Figure 28).

The ratio of 260/230 is another indicator of DNA purity. In our experiments, DNA eluted from polyacrylamide gel always produced a strong peak at 230 nm (Figure 28). It's likely due to the presence of Tris molecules that had diffused from the gel and the TBE buffer, supporting the need for further purification of the eluted aptamers.[85]

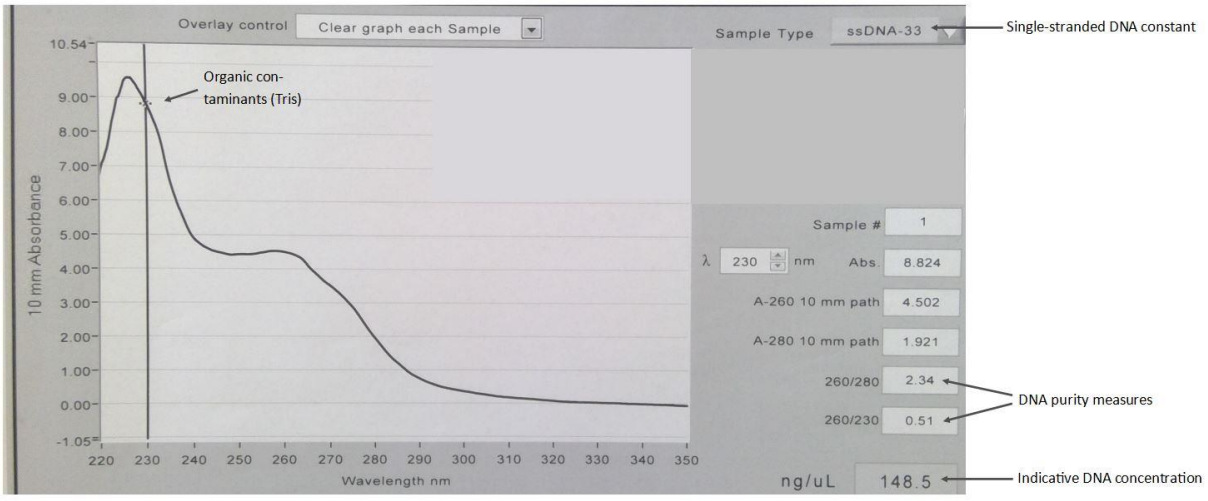

Figure 28. A representative DNA quantity and quality determination with NanoDrop spectrophotometer.

3.5. Selected aptamers neutralisation efficacy.

To investigate the selected aptamers neutralisation capacity following the second round of SELEX, ELISA was performed against cN1A protein challenged with anti-cN1A antibodies with and without the aptamers addition. Bound anti-cN1A were detected with goat anti-human IgG, IgM, IgA antibodies.

In the first experiment, anti-cN1A antibodies were pre-incubated with increasing concentrations of aptamers for one hour at room temperature. Then, the ELISA was performed following the standard protocol. In line with my hypothesis, I was expecting to observe the reduction in anti-cN1A binding as detected by the decrease in ELISA absorbance values. However, upon the aptamer addition, the absorbance remained unchanged or increased (Figure 29). The increase was dose-dependent until the plateau was reached at 12.5 pM.

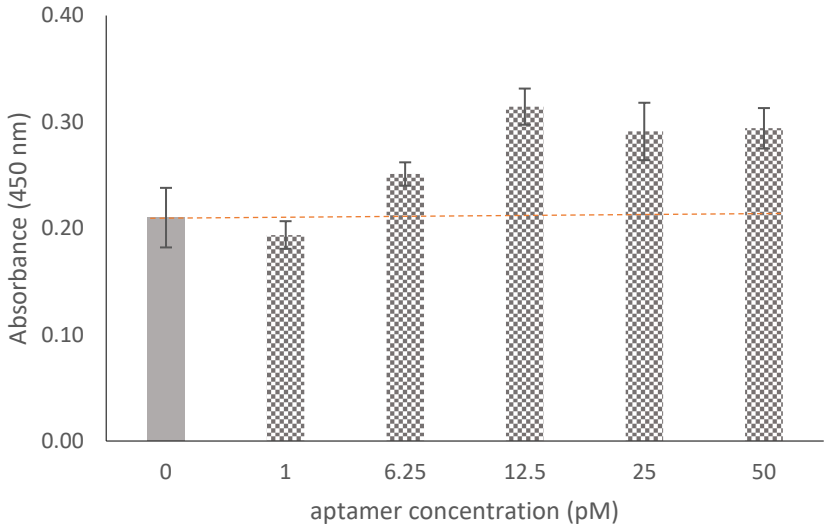

Figure 29. ELISA investigating aptamer neutralisation efficacy. Anti-cN1A was pre-incubated with increasing concentrations of aptamers up to 50 pM prior to the addition to cN1A-coated wells (20 µg/mL) for one hour at room temperature. Goat anti-human-IgG/A/M antibodies were used for detection. Each anti-cN1A:aptamer ratio was assayed in triplicate. Columns represent mean absorbance values. Error bars represent standard deviation.

While unexpected, this data could result from the selected aptamers exclusively blocking monomeric immunoglobulins, either IgG or IgA (mostly monomeric in serum). In theory, blocking of these antibodies could change the composition of the primary bound immunoglobulins in each ELISA well by increasing the proportion of multimeric IgM.

Given that IgM consists of five subunits, it is theoretically able to conjugate with five times more secondary antibodies than IgG or IgA potentially increasing the endpoint absorbance values.

This hypothesis relies on two assumptions. Firstly, some low-affinity anti-cN1A must remain unbound in the ELISA well after two-hour incubation under our conditions. Secondly, aptamer blocking of IgM anti-cN1A must be insufficient to prevent their interaction with cN1A protein.

I have demonstrated in the previous experiment (Figure 18) that the absorbance of 0.2 corresponds to incomplete clearance of antibodies from the solution by cN1A at 20 μg/mL. From this, it can be extrapolated that excess low-affinity unbound antibodies may be present in the ELISA wells, even though it has not been empirically demonstrated in this experiment.

Regarding the second assumption, it is possible that aptamers that were capable of binding IgM were eliminated from the selection pool. If some of the IgM subunits remained unblocked during the SELEX, the entire immunoglobulin could be captured by the target protein and avoid recovery in the supernatant for selection.

To assess whether the selected aptamers blocking efficacy could be improved, another experiment was carried out where the aptamer incubation with anti-cN1A was increased from one hour to overnight. The ELISA was performed as before following the standard protocol. Indeed, upon prolonged incubation, I observed a decrease in the final absorbance value of 25% for all antibody isotypes and 27% for IgG only (Figure 30). Using the data obtained from a

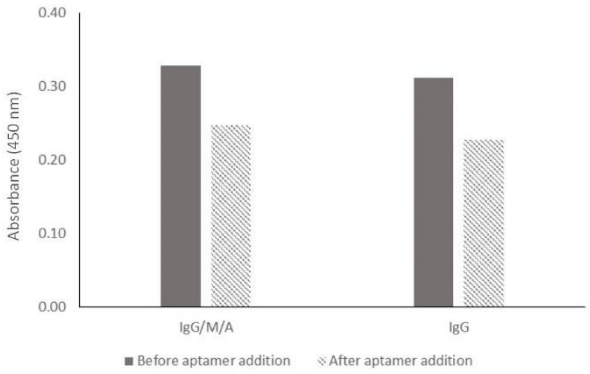

Figure 30. ELISA investigating aptamer neutralisation efficacy. Anti-cN1A was pre-incubated with 15 pM aptamers overnight at 4°C prior to the addition to cN1A-coated wells (20 μg/mL). Goat anti-IgG/M/A and anti-IgG antibodies were used for detection. Each condition was assayed once.

previous experiment (see Section 3.3.1), a standard absorbance curve was constructed (Figure 31). The standard curve was fitted with a polynomial equation used to calculate the concentration

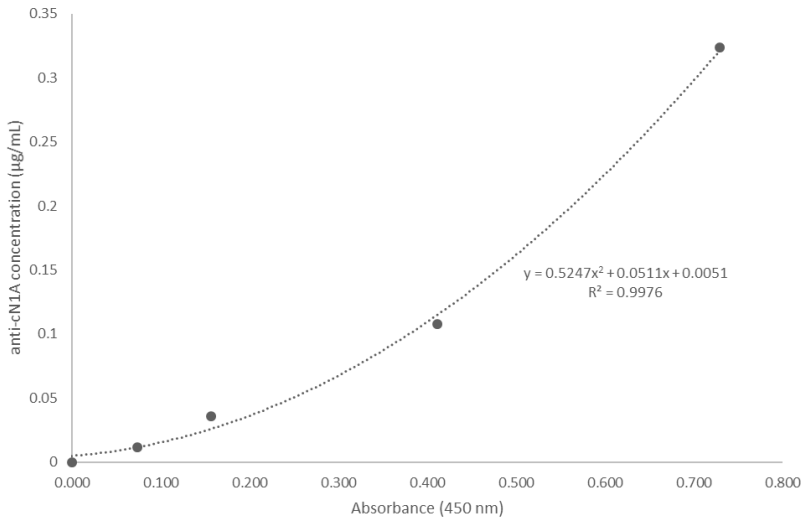

Figure 31. ELISA was performed with serially titrated anti-cN1A incubated for two hours at room temperature in wells coated with 20 µg/mL cN1A protein. Bound antibodies were detected with goat anti-human horseradish peroxidase (HRP)-conjugated antibodies against IgG/M/A and visualised via TMB substrate reaction at 450 nm. Mean of duplicate measurements are plotted and fitted with a polynomial trendline following the equation $y=0.5247x^2+0.0511x+0.0051$

of bound antibodies of all isotypes before and after the aptamer addition. It was determined that 35% of anti-cN1A were neutralised following the overnight incubation with the selected aptamers. This data suggests that the aptamers selected after two cycles of SELEX may have low affinity against a subpopulation of anti-cN1A, possibly of IgM isotype. After prolonged incubation, even these low-affinity binders are capable of neutralising anti-cN1A interaction with their target protein.

In future experiments, we will address the issue of the initial selection against IgM by isolating them from the anti-cN1A pool with streptavidin magnetic beads conjugated to biotinylated anti-human-IgM antibodies. Once isolated, IgM will be fragmented into IgG-like subunits of 200 kDa using trypsin or 2-mercaptoethylamine (Figure 32). The selection from the initial aptamer pool will then be repeated to yield blockers against such fragmented IgM subunits.

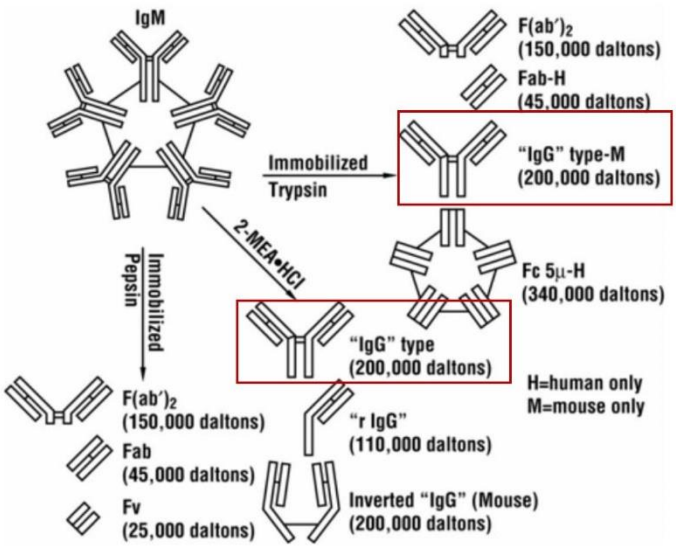

Figure 32. IgM fragments generated using trypsin, pepsin or 2-mercaptoethylamine. Image adapted from: Thermo Scientific.

CHAPTER 4. Conclusion: aims achieved, lessons learnt and future directions.

The work outlined in this thesis was aimed at selecting DNA aptamers that prevent binding of anti-cytosolic 5'-nucleotidase-1A antibodies to their target protein. The current knowledge of anti-cN1A antibodies' structure is limited. Consistent with our findings, previous studies have demonstrated that the antibodies are polyclonal, meaning they target a variety of cN1A epitopes, and they exist as different isotypes. The selection against such a heterogenous immunoglobulin pool inevitably adds complexity to an already complex and variable process. Nonetheless, targeting multiple binding sites may increase the chances of obtaining effective aptamers as a result of SELEX.

As an additional obstacle, the target antibodies are not readily available. The only way to obtain anti-cN1A was to purify them from a seropositive IBM patient's serum. Considering the advanced age and the declining health of many of the IBM patients in our cohort, it was challenging to obtain adequate amount of blood for purification. Nevertheless, we were fortunate to engage a patient with high antibody titres who was able to donate a sufficient volume of blood for this study. The purification methodology using magnetic beads was developed by modifying the manufacturer's protocol. Once the methodology was established, repeated cycles of purification resulted in the isolation of 6.5 mg of anti-cN1A. This quantity was in excess of what was required for SELEX, therefore a large fraction of the purified antibodies was biobanked for future research.

The selection methodology utilised in this work was based on the modified cyclical process of systematic evolution of ligands by exponential enrichment, otherwise known as SELEX. The method combines sequential stages of separating binding aptamers from the initial pool, amplifying the selected aptamers and creating a new aptamer pool by segregating and purifying the oligonucleotides. Similar to the natural selection of species, the strongest binders are enriched within the selection library at every cycle until only the most effective aptamers remain.

During this project, two selection cycles were completed. The first cycle was markedly challenging because every step required development and optimisation. Due to a significant loss of aptamers during the purification from polyacrylamide gel in the first round, insufficient DNA was remaining to carry over into the next SELEX cycle. Therefore, the first cycle was repeated using the initial library as the selection template. The number of amplification reactions was increased to ensure that an adequate amount of single-stranded DNA was obtained at the end of the cycle. The amplified binders from the repeated first cycle were combined with the binders selected previously and carried over to the following SELEX cycle. This way ensured that no effective aptamers were lost. Furthermore, a small amount of aptamers from each selection round was retained as a safeguard in case of a failed cycle guaranteeing that the SELEX process can be restarted from that cycle.

At the end of the first round of SELEX, a total of 3,150 ng of ssDNA as measured by NanoDrop was obtained and taken forward to the next stage of selection. Following the capture SELEX, 222 ng of ssDNA (7%) was retained. This result suggested that the screening method for neutralising aptamers was sufficiently stringent for the early cycles of SELEX.

While I was successful in isolating some aptamers after two rounds of selection, it is yet to be determined whether these oligonucleotides are specific for anti-cN1A. To improve the aptamers specificity, the third SELEX cycle and every other cycle after that will include a counter-selection step. The purpose of counter-selection is to remove any non-specific binders by incubating the aptamer pool with unrelated molecules, such as magnetic beads and secondary antibodies. At later stages of SELEX, the counter-selection will also include incubation with non-targeted human serum proteins. For this, the coating of an ELISA plate will be performed with human sera precleared from anti-cN1A immunoglobulins. The selected aptamers will then be incubated with the well-immobilised proteins allowing any non-specific aptamers to bind. The supernatant containing specific aptamers will be retained and used for further selection.

To assess the neutralising capacity of the selected aptamers, an ELISA was carried out where aptamer-blocked antibodies were challenged with immobilised cN1A. While the resultant absorbance values were expected to decrease with increasing aptamer concentration due to less anti-cN1A binding their target, I instead observed a dose-dependent increase in absorbance. I hypothesise that this result was due to the increased fraction of bound IgM that carry multiple binding sites for secondary antibodies prompting an increase in absorbance compared to the IgG and IgA-dominated antibody pool. This result strongly indicated that the selected aptamers have neutralising efficacy against IgG and IgA anti-cN1A. By increasing aptamer-antibody incubation time, we were able to demonstrate a 35% reduction in antibody-binding to cN1A suggesting that the selected aptamers carry neutralising capacity but have low avidity for anti-cN1A. I feel positive that ongoing selection following the established methodology will lead us to the development of aptamers with higher affinity and avidity for anti-cN1A immunoglobulins. Carrying out the selection against fragmented IgM will additionally increase the fraction of immunoglobulins against which the aptamers have blocking capacity.

Extending this work, we plan to characterise the selected aptamers and evaluate their efficacy against anti-cN1A antibodies isolated from other IBM patients in the hope that they have broad neutralisation capacity. Furthermore, the generated aptamers will be modified for *in vivo* delivery and evaluated in a pre-clinical mouse model. Ultimately, we expect to advance the aptamers to human clinical trials with the aim to produce a novel therapeutic for anti-cN1A-positive IBM patients.

References.

1. Dalakas MC. Inflammatory Muscle Diseases. N Engl J Med. 2015;373(4):393-4.

2. Greenberg SA. Theories of the pathogenesis of inclusion body myositis. Curr Rheumatol Rep. 2010;12(3):221-8.

3. Griggs RC, Askanas V, DiMauro S, Engel A, Karpati G, Mendell JR, et al. Inclusion body myositis and myopathies. Ann Neurol. 1995;38(5):705-13.

4. Kramp SL, Karayev D, Shen G, Metzger AL, Morris RI, Karayev E, et al. Development and evaluation of a standardized ELISA for the determination of autoantibodies against cN-1A (Mup44, NT5C1A) in sporadic inclusion body myositis. Auto Immun Highlights. 2016;7(1):16.

5. Benveniste O, Guiguet M, Freebody J, Dubourg O, Squier W, Maisonobe T, et al. Long-term observational study of sporadic inclusion body myositis. Brain. 2011;134(Pt 11):3176-84.

6. Goyal NA, Cash TM, Alam U, Enam S, Tierney P, Araujo N, et al. Seropositivity for NT5c1A antibody in sporadic inclusion body myositis predicts more severe motor, bulbar and respiratory involvement. J Neurol Neurosurg Psychiatry. 2016;87(4):373-8.

7. Badrising UA, Maat-Schieman M, van Duinen SG, Breedveld F, van Doorn P, van Engelen B, et al. Epidemiology of inclusion body myositis in the Netherlands: a nationwide study. Neurology. 2000;55(9):1385-7.

8. Dobloug GC, Antal EA, Sveberg L, Garen T, Bitter H, Stjarne J, et al. High prevalence of inclusion body myositis in Norway; a population-based clinical epidemiology study. Eur J Neurol. 2015;22(4):672-e41.

9. Suzuki N, Aoki M, Mori-Yoshimura M, Hayashi YK, Nonaka I, Nishino I. Increase in number of sporadic inclusion body myositis (sIBM) in Japan. J Neurol. 2012;259(3):554-6.

10. Phillips BA, Zilko PJ, Mastaglia FL. Prevalence of sporadic inclusion body myositis in Western Australia. Muscle Nerve. 2000;23(6):970-2.

11. Needham M, Corbett A, Day T, Christiansen F, Fabian V, Mastaglia FL. Prevalence of sporadic inclusion body myositis and factors contributing to delayed diagnosis. Journal of Clinical Neuroscience. 2008;15(12):1350-3.

12. Benveniste O, Stenzel W, Hilton-Jones D, Sandri M, Boyer O, van Engelen BG. Amyloid deposits and inflammatory infiltrates in sporadic inclusion body myositis: the inflammatory egg comes before the degenerative chicken. Acta Neuropathol. 2015;129(5):611-24.

13. van der Meulen MF, Bronner IM, Hoogendijk JE, Burger H, van Venrooij WJ, Voskuyl AE, et al. Polymyositis: an overdiagnosed entity. Neurology. 2003;61(3):316-21.

14. Rose MR, Jones K, Leong K, Walter MC, Miller J, Dalakas MC, et al. Treatment for inclusion body myositis. Cochrane Database of Systematic Reviews. 2015;2015(6).

15. Benveniste O, Benveniste O, Rider LG, Rider LG, Aggarwal R, Allenbach Y, et al. 213th ENMC International Workshop: Outcome measures and clinical trial readiness in idiopathic inflammatory myopathies, Heemskerk, The Netherlands, 18–20 September 2015. Neuromuscular Disorders. 2016;26(8):523-34.

16. Lundberg IE, Tjärnlund A, Bottai M, Werth VP, Pilkington C, Visser Md, et al. 2017 European League Against Rheumatism/American College of Rheumatology classification

criteria for adult and juvenile idiopathic inflammatory myopathies and their major subgroups. Annals of the Rheumatic Diseases. 2017;76(12):1955-64.

17. Nutt SL, Hodgkin PD, Tarlinton DM, Corcoran LM. The generation of antibody-secreting plasma cells. Nature Reviews Immunology. 2015;15(3):160-71.

18. Coico Ra, Sunshine Ga. Immunology: a short course. Seventh;7; ed. Chichester, West Sussex, UK;Hoboken, NJ;: John Wiley & Sons Inc; 2015.

19. Schmidt K, Mueller-Eckhardt C. Antinuclear autoantibodies of IgD class. An analysis of 82 patients. Z Immunitatsforsch Exp Klin Immunol. 1973;145(5):385-91.

20. Wu Y, Chen W, Chen H, Zhang L, Chang Y, Yan S, et al. The Elevated Secreted Immunoglobulin D Enhanced the Activation of Peripheral Blood Mononuclear Cells in Rheumatoid Arthritis. PLoS One. 2016;11(1):e0147788.

21. Perricone Ce, Shoenfeld Ye. Mosaic of autoimmunity: the novel factors of autoimmune diseases. London, England: Academic Press; 2019.

22. Aletaha D, Neogi T, Silman AJ, Funovits J, Felson DT, Bingham CO, 3rd, et al. 2010 Rheumatoid arthritis classification criteria: an American College of Rheumatology/European League Against Rheumatism collaborative initiative. Arthritis Rheum. 2010;62(9):2569-81.

23. Sherer Y, Gorstein A, Fritzler MJ, Shoenfeld Y. Autoantibody explosion in systemic lupus erythematosus: more than 100 different antibodies found in SLE patients. Semin Arthritis Rheum. 2004;34(2):501-37.

24. Chen Y, Park YB, Patel E, Silverman GJ. IgM antibodies to apoptosis-associated determinants recruit C1q and enhance dendritic cell phagocytosis of apoptotic cells. J Immunol. 2009;182(10):6031-43.

25. Mageed RA, Børretzen M, Moves SP, Thompson KM, Natvig JB. Rheumatoid factor autoantibodies in health and disease. Annals of the New York Academy of Sciences. 1997;815(1 B-Lymphocytes):296-311.

26. Jonsson R, Theander E, Sjöström B, Brokstad K, Henriksson G, Klinisk mikrobiologi M, et al. Autoantibodies Present Before Symptom Onset in Primary Sjögren Syndrome. JAMA. 2013;310(17):1854-5.

27. Arahata K, Engel AG. Monoclonal antibody analysis of mononuclear cells in myopathies. I: Quantitation of subsets according to diagnosis and sites of accumulation and demonstration and counts of muscle fibers invaded by T cells. Ann Neurol. 1984;16(2):193-208.

28. Greenberg SA, Bradshaw EM, Pinkus JL, Pinkus GS, Burleson T, Due B, et al. Plasma cells in muscle in inclusion body myositis and polymyositis. Neurology. 2005;65(11):1782-7.

29. Bradshaw EM, Orihuela A, McArdel SL, Salajegheh M, Amato AA, Hafler DA, et al. A Local Antigen-Driven Humoral Response Is Present in the Inflammatory Myopathies. The Journal of Immunology. 2007;178(1):547-56.

30. Bradshaw EM, Orihuela A, McArdel SL, Salajegheh M, Amato AA, Hafler DA, et al. A local antigen-driven humoral response is present in the inflammatory myopathies. J Immunol. 2007;178(1):547-56.

31. Durie FH, Foy TM, Masters SR, Laman JD, Noelle RJ. The role of CD40 in the regulation of humoral and cell-mediated immunity. Immunol Today. 1994;15(9):406-11.

32. Ray A, Amato AA, Bradshaw EM, Felice KJ, DiCapua DB, Goldstein JM, et al. Autoantibodies Produced at the Site of Tissue Damage Provide Evidence of Humoral Autoimmunity in Inclusion Body Myositis. PLoS ONE. 2012;7(10):e46709.

33. Salajegheh M, Lam T, Greenberg SA. Autoantibodies against a 43 KDa muscle protein in inclusion body myositis. PLoS One. 2011;6(5):e20266.

34. Larman HB, Salajegheh M, Nazareno R, Lam T, Sauld J, Steen H, et al. Cytosolic 5'-nucleotidase 1A autoimmunity in sporadic inclusion body myositis. Ann Neurol. 2013;73(3):408-18.

35. Pluk H, van Hoeve BJ, van Dooren SH, Stammen-Vogelzangs J, van der Heijden A, Schelhaas HJ, et al. Autoantibodies to cytosolic 5'-nucleotidase 1A in inclusion body myositis. Ann Neurol. 2013;73(3):397-407.

36. Herbert MK, Stammen-Vogelzangs J, Verbeek MM, Rietveld A, Lundberg IE, Chinoy H, et al. Disease specificity of autoantibodies to cytosolic 5'-nucleotidase 1A in sporadic inclusion body myositis versus known autoimmune diseases. Ann Rheum Dis. 2016;75(4):696-701.

37. Bianchi V, Spychala J. Mammalian 5'-nucleotidases. J Biol Chem. 2003;278(47):46195-8.

38. Hunsucker SA, Spychala J, Mitchell BS. Human cytosolic 5′-nucleotidase I: Characterization and role in nucleoside analog resistance. Journal of Biological Chemistry. 2001;276(13):10498-504.

39. Kviklyte S, Vertommen D, Yerna X, Andersen H, Xu X, Gailly P, et al. Effects of genetic deletion of soluble 5'-nucleotidases NT5C1A and NT5C2 on AMPK activation and nucleotide levels in contracting mouse skeletal muscles. Am J Physiol Endocrinol Metab. 2017;313(1):E48-E62.

40. Carling D, Mayer FV, Sanders MJ, Gamblin SJ. AMP-activated protein kinase: nature's energy sensor. Nat Chem Biol. 2011;7(8):512-8.

41. Tawara N, Yamashita S, Zhang X, Korogi M, Zhang Z, Doki T, et al. Pathomechanisms of anti-cytosolic 5'-nucleotidase 1A autoantibodies in sporadic inclusion body myositis. Ann Neurol. 2017;81(4):512-25.

42. Greenberg SA. Cytoplasmic 5'-nucleotidase autoantibodies in inclusion body myositis: Isotypes and diagnostic utility. Muscle Nerve. 2014;50(4):488-92.

43. Lilleker JB, Rietveld A, Pye SR, Mariampillai K, Benveniste O, Peeters MT, et al. Cytosolic 5'-nucleotidase 1A autoantibody profile and clinical characteristics in inclusion body myositis. Ann Rheum Dis. 2017;76(5):862-8.

44. Felice KJ, Whitaker CH, Wu Q, Larose DT, Shen G, Metzger AL, et al. Sensitivity and clinical utility of the anti-cytosolic 5'-nucleotidase 1A (cN1A) antibody test in sporadic inclusion body myositis: Report of 40 patients from a single neuromuscular center. Neuromuscul Disord. 2018;28(8):660-4.

45. Lloyd TE, Christopher-Stine L, Pinal-Fernandez I, Tiniakou E, Petri M, Baer A, et al. Cytosolic 5'-Nucleotidase 1A As a Target of Circulating Autoantibodies in Autoimmune Diseases. Arthritis Care Res (Hoboken). 2016;68(1):66-71.

46. Muro Y, Nakanishi H, Katsuno M, Kono M, Akiyama M. Prevalence of anti-NT5C1A antibodies in Japanese patients with autoimmune rheumatic diseases in comparison with other patient cohorts. Clin Chim Acta. 2017;472:1-4.

47. Amlani A, Choi MY, Tarnopolsky M, Brady L, Clarke AE, Garcia-De La Torre I, et al. Anti-NT5c1A Autoantibodies as Biomarkers in Inclusion Body Myositis. FRONTIERS IN IMMUNOLOGY. 2019;10:745-.

48. Rietveld A, van den Hoogen LL, Bizzaro N, Blokland SLM, Daehnrich C, Gottenberg JE, et al. Autoantibodies to Cytosolic 5 '-Nucleotidase 1A in Primary Sjogren's Syndrome and Systemic Lupus Erythematosus. FRONTIERS IN IMMUNOLOGY. 2018;9:1200.

49. Kanwar JR, Roy K, Maremanda NG, Subramanian K, Veedu RN, Bawa R, et al. Nucleic acid-based aptamers: applications, development and clinical trials. Curr Med Chem. 2015;22(21):2539-57.

50. Doudna JA, Cech TR, Sullenger BA. Selection of an RNA Molecule that Mimics a Major Autoantigenic Epitope of Human Insulin Receptor. Proceedings of the National Academy of Sciences of the United States of America. 1995;92(6):2355-9.

51. Wolter O, Mayer G. Aptamers as Valuable Molecular Tools in Neurosciences. The Journal of Neuroscience. 2017;37(10):2517-23.

52. Ellington AD, Szostak JW. In vitro selection of RNA molecules that bind specific ligands. Nature. 1990;346(6287):818-22.

53. Tuerk C, Gold L. Systematic evolution of ligands by exponential enrichment: RNA ligands to bacteriophage T4 DNA polymerase. Science. 1990;249(4968):505-10.

54. Robertson DL, Joyce GF. Selection in vitro of an RNA enzyme that specifically cleaves single-stranded DNA. Nature. 1990;344(6265):467-8.

55. Ellington AD, Szostak JW. Selection in vitro of single-stranded DNA molecules that fold into specific ligand-binding structures. Nature. 1992;355(6363):850-2.

56. Tuerk C, MacDougal S, Gold L. RNA Pseudoknots that Inhibit Human Immunodeficiency Virus Type 1 Reverse Transcriptase. Proceedings of the National Academy of Sciences of the United States of America. 1992;89(15):6988-92.

57. Balogh Z, Lautner G, Bardoczy V, Komorowska B, Gyurcsanyi RE, Meszaros T. Selection and versatile application of virus-specific aptamers. FASEB J. 2010;24(11):4187-95.

58. Tan W, Donovan MJ, Jiang J. Aptamers from cell-based selection for bioanalytical applications. Chem Rev. 2013;113(4):2842-62.

59. Vorobyeva M, Timoshenko V, Vorobjev P, Venyaminova A. Aptamers Against Immunologic Targets: Diagnostic and Therapeutic Prospects. Nucleic Acid Ther. 2016;26(1):52-65.

60. Tsai DE, Kenan DJ, Keene JD. In vitro selection of an RNA epitope immunologically cross-reactive with a peptide. Proc Natl Acad Sci U S A. 1992;89(19):8864-8.

61. Darmostuk M, Rimpelova S, Gbelcova H, Ruml T. Current approaches in SELEX: An update to aptamer selection technology. Biotechnology Advances. 2015;33(6):1141-61.

62. Wang T, Chen C, Larcher LM, Barrero RA, Veedu RN. Three decades of nucleic acid aptamer technologies: Lessons learned, progress and opportunities on aptamer development. Biotechnol Adv. 2019;37(1):28-50.

63. Stoltenburg R, Reinemann C, Strehlitz B. SELEX--a (r)evolutionary method to generate high-affinity nucleic acid ligands. Biomol Eng. 2007;24(4):381-403.

64. Lee S-W, Sullenger BA. Isolation of a nuclease-resistant decoy RNA that selectively blocks autoantibody binding to insulin receptors on human lymphocytes. Journal of Experimental Medicine. 1996;184(2):315-24.

65. Vorobjeva MA, Krasitskaya VV, Fokina AA, Timoshenko VV, Nevinsky GA, Venyaminova AG, et al. RNA aptamer against autoantibodies associated with multiple sclerosis and bioluminescent detection probe on its basis. Analytical Chemistry. 2014;86(5):2590-4.

66. Kim Y-M, Choi KH, Jang Y-J, Yu J, Jeong S. Specific modulation of the anti-DNA autoantibody–nucleic acids interaction by the high affinity RNA aptamer. Biochemical and Biophysical Research Communications. 2003;300(2):516-23.

67. Lee S-W, Sullenger BA. Isolation of a nuclease-resistant decoy RNA that can protect human acetylcholine receptors from myasthenic antibodies. Nature Biotechnology. 1997;15(1):41-5.

68. Seo HS, Lee SW. In vitro selection of the 2'-fluoro-2'-deoxyribonucleotide decoy RNA inhibitor of myasthenic autoantibodies. Journal of Microbiology and Biotechnology. 2000;10(5):707-13.

69. Haberland A, Holtzhauer M, Schlichtiger A, Bartel S, Schimke I, Müller J, et al. Aptamer BC 007 – A broad spectrum neutralizer of pathogenic autoantibodies against G-protein-coupled receptors. European Journal of Pharmacology. 2016;789:37-45.

70. Berlin Cures completes phase 1 study of BC 007 for cardiomyopathy treatment. PharmaBiz. 2018.

71. Bundell C, Shakya R, Brusch A, McLean Tooke A, Hollingsworth P, Needham M. Diagnostic utility of cytoplasmic 5’-nucleotidase autoantibodies to identify inclusion body myositis patients. Pathology. 2017;49:S112-S3.

72. Bornhorst JA, Falke JJ. Purification of proteins using polyhistidine affinity tags. Methods Enzymol. 2000;326:245-54.

73. Chen L, Yu Z, Lee Y, Wang X, Zhao B, Jung YM. Quantitative evaluation of proteins with bicinchoninic acid (BCA): resonance Raman and surface-enhanced resonance Raman scattering-based methods. Analyst. 2012;137(24):5834-8.

74. Wang MS, Reed SM. Direct visualization of electrophoretic mobility shift assays using nanoparticle-aptamer conjugates. Electrophoresis. 2012;33(2):348-51.

75. Zhang Z, Oni O, Liu J. New insights into a classic aptamer: Binding sites, cooperativity and more sensitive adenosine detection. Nucleic Acids Research. 2017;45(13):7593-601.

76. Stayton PS, Freitag S, Klumb LA, Chilkoti A, Chu V, Penzotti JE, et al. Streptavidin-biotin binding energetics. Biomol Eng. 1999;16(1-4):39-44.

77. Mullis K, Faloona F, Scharf S, Saiki R, Horn G, Erlich H. Specific enzymatic amplification of DNA in vitro: the polymerase chain reaction. Cold Spring Harb Symp Quant Biol. 1986;51 Pt 1:263-73.

78. Hestand MS, Van Houdt J, Cristofoli F, Vermeesch JR. Polymerase specific error rates and profiles identified by single molecule sequencing. Mutat Res. 2016;784-785:39-45.

79. Tolle F, Wilke J, Wengel J, Mayer G. By-product formation in repetitive PCR amplification of DNA libraries during SELEX. PLoS One. 2014;9(12):e114693.

80. Marshall KA, Ellington AD. Molecular Parasites That Evolve Longer Genomes. Journal of Molecular Evolution. 1999;49(5):656-63.

81. Maxam AM, Gilbert W. A New Method for Sequencing DNA. Proceedings of the National Academy of Sciences of the United States of America. 1977;74(2):560-4.

82. Fadouloglou VE. Electroelution of nucleic acids from polyacrylamide gels: A custom-made, agarose-based electroeluter. Analytical Biochemistry. 2013;437(1):49-51.

83. Smith HO. Recovery of DNA from gels. Methods Enzymol. 1980;65(1):371-80.

84. Pollard J. Purification of oligonucleotides using denaturing polyacrylamide gel electrophoresis.1998 30/08/2019. Available from: https://molbio.mgh.harvard.edu/szostakweb/protocols/denaturepage/index.html.

85. Carmack M, Leavitt JJ. The Ultraviolet Absorption Spectra of tris-(Hydroxymethyl)-methylnitrosohydroxylamine, tris-(Hydroxymethyl)-methylnitramine, and their Salts. Journal of the American Chemical Society. 1949;71(4):1221-3.